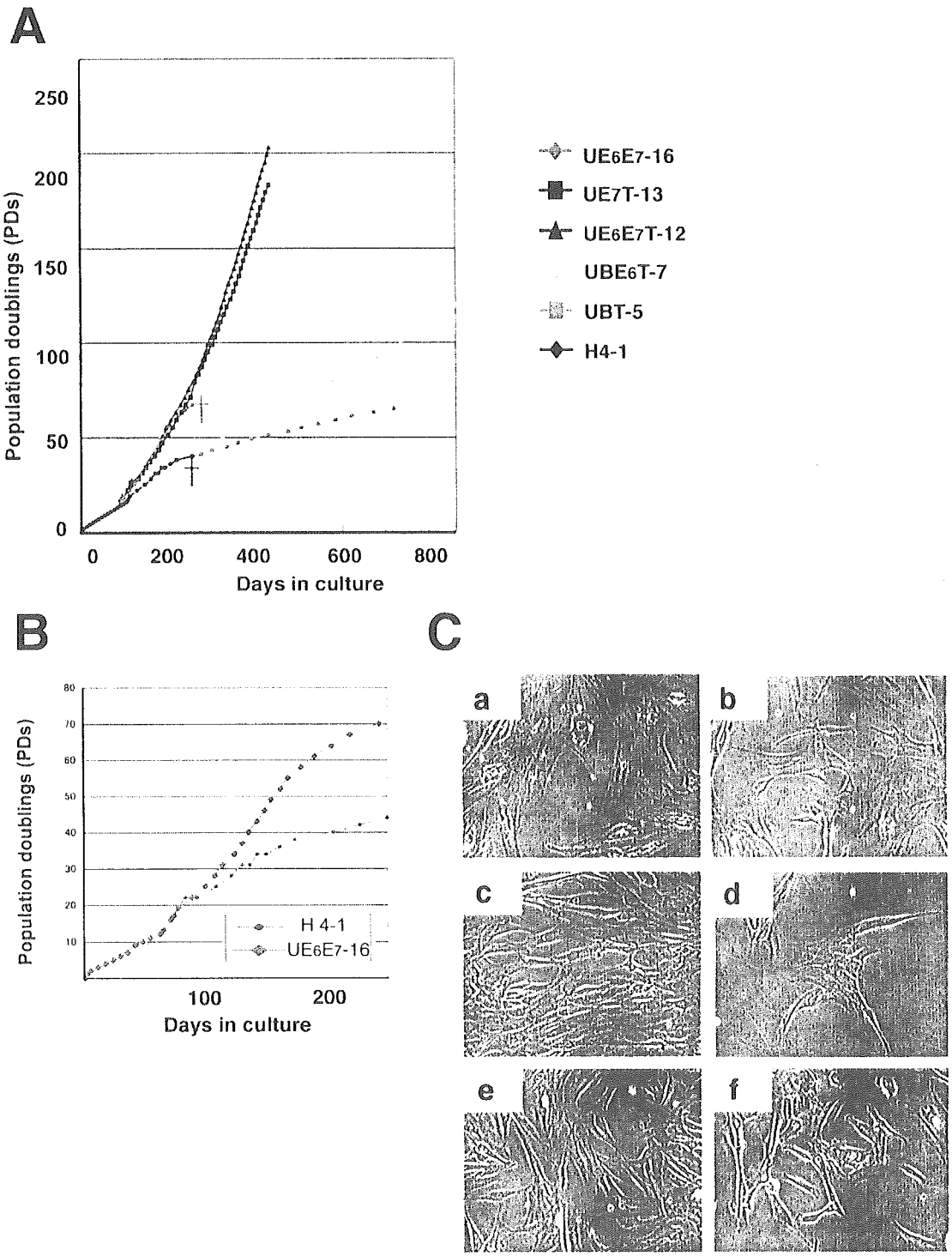

FIG. 1. In vitro growth of parental and transduced strains of bone marrow stromal cells. (A) The population doublings of UE6E7-16, UE7T-13, UE6E7T-12, UBE6T-7, UBT-5, and H4-1 cells are shown. UE7T-13, UE6E7T-12, UBE6T-7, and UBT-5 cells proliferated for over 60 PDs and for more than 400 days. By contrast, parental H4-1 cells and UE6E7-16 cells stopped growing and entered senescence or the growth arrest stage, which is indicated by crosses. (B) H4-1 and UE6E7-16 cells entered senescence at 44 PDs and 70 PDs, respectively, approximately 200 days after the start of culture. (C) Phase-contrast photomicrographs of the bone marrow stromal cells at the semiconfluent stage in a 40-PD culture. (a) H4-1 cells; (b) UBT-5 cells; (c) UBE6T-7 cells; (d) UE6E7T-12 cells; (e) UE7T-13 cells; (f) UE6E7-16 cells.

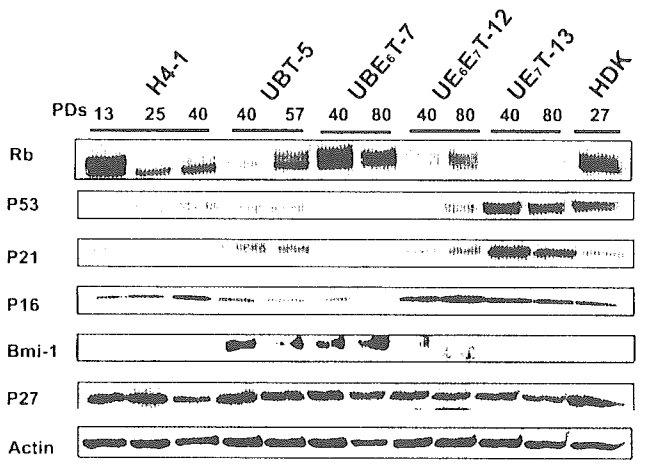

FIG. 2. Time course analysis of cell cycle-associated protein levels in cells with an extended life span. Cell cycle-associated proteins, i.e., Rb, p53, p21, p16, Bmi-1, and p27, in UBT-5, UBE6T-7, UE6E7T-12, UE7T-13, and H4-1 cells were analyzed by Western blotting. Cells cultured for the PDs indicated were assayed. The expression pattern was reproducibly observed in four separate experiments. Expression of actin protein was monitored as a loading control.

of UBT-5, UBE6T-7, UE6E7T-12, and UE7T-13 cells was maintained irrespective of the PD number (Fig. 3B, C, and D).

Karyotypic analysis of parental and transduced cells with extended life spans. We performed a karyotypic analysis (G banding and SKY) of both the parental stromal cells (H4-1) and the cells transduced with hTERT and *bmi-1*, E6, or E7 (see Materials and Methods). SKY permits a detailed analysis of all complex markers and provides insights into their involvement in subsequent rearrangements (34). Our studies raised some interesting points concerning chromosomal abnormality. No genomic abnormalities were found in the parental cells, but an increase in chromosomal number appeared in the other strains, as shown by G-banding and SKY analyses (Table 1 and Fig. 4), except for in the UE7T-13 cells. These abnormalities included translocations, a deletion, other rearrangements, and polyploidy. Surprisingly, we found no genomic changes in the UE7T-13 cells at over 120 PDs.

Establishment of a novel protocol for neuroectodermal differentiation of human marrow stromal cells. Murine stromal cells have been reported to have been transdifferentiated into neuronal lineages (6, 16, 22) by several different protocols. In this study, we devised a simple protocol for neuroectodermal differentiation from mesoderm-derived cells (Fig. 5A). Briefly, growing, adherent stromal cells were trypsinized and pelleted down by centrifugation, and after as much growth medium as possible was aspirated, the pelleted cell aggregates were pipetted with a 20-μl microtip. Each cell aggregate was then replated onto a laminin-coated coverslip in a 7-mm-diameter 24-well culture dish (Fig. 5A), and the growth medium was replaced with B27-supplemented growth medium containing NGF, BDNF, and bFGF. Cells not subjected to this protocol have fibroblast morphology (Fig. 5B, a). The shape of the stromal cells began to change on day 7 after replating, and the cells did not adhere to adjacent cells. The cells then started to exhibit neuron-like morphology that included a refractile round cell body, a neurite-like process(es), and a triangular axon terminal(s) (Fig. 5B, b to d). By days 14 to 21, more than 80% of the bone marrow cells had formed neurite-like processes and exhibited neuron-like morphology. All experiments were repeated at least 10 times using different population doublings (20 to 100 PDs) before using the cells for neuroectoderm differentiation.

Expression of neuron-specific proteins during neuroectodermal differentiation of human marrow stromal cells. After induction, the UBT-5, UBE6T-7, UE6E7T-12, and UE7T-13 cells became positive for the neuron-specific markers microtubule-associated protein 2 (MAP-2), tubulin 3, and Nurr1 (Fig. 5C, a, c, d, k, and n), implying that they could be induced into neuronal lineages. More than 80% of all the tested cells were positive for MAP-2 and Nurr1, but no staining was detected with antibodies against GFAP (an astrocyte-specific marker) or O4 (an oligodendrocyte-specific marker) (data not shown). Undifferentiated UE7T-13 and H4-1 cells did not exhibit neuroectodermal characteristics (Fig. 5C, b and l).

Gene chip analysis during neuroectodermal differentiation. To clarify the specific gene expression profile of human marrow stromal cells, we compared the expression levels of approximately 23,000 genes by neuronally differentiated UE7T-13 cells, undifferentiated UE7T-13 cells, and parental H4-1 cells (GEO accession number GSE2110 [http://1954.jukuin.keio.ac.jp/umezawa/chip/mori]) using the Affymetrix gene chip oligonucleotide arrays. Of the approximately 23,000 genes represented on the gene chip, 2,123 genes were up-regulated to more than twice their expression level in undifferentiated cells. Genes whose expression increased or decreased are shown in Table 2. The Nurr1, kynureninase, apolipoprotein, RARRES1, ABC1, rab27B, STC1, WISP2, rhoGAP6, SLC2A5, and palmderphin genes were among the top 0.1% in terms of increase in expression. Surprisingly, expression of Nurr1/NR4A2, which is essential for differentiation of the nigral dopaminergic neurons (23, 32), was up-regulated 26.1-fold. Wnt-5a promotes the acquisition of dopaminergic neurons (8), and its expression was increased 7.1-fold. These findings imply that the characteristics of these cells are similar to those of midbrain neurons. The dendrogram analysis clearly showed that the change in gene expression pattern is dramatic and neuron specific during neuroectodermal differentiation rather than being leaky, subtle, and nonspecific (Fig. 6).

Expression of neuron-specific genes in differentiated UE7T-13 cells. To confirm the global change in gene expression during neuronal differentiation, RT-PCR was performed with primers that specifically react with human neuronal genes. Differentiated UBT-5, UBE6T-7, UE6E7T-12, UE7T-13, UE6E7-16, and H4-1 cells expressed Nurr1, MAP2, tubulin 3, medium-size neurofilament (NF-M), Sox-2, and nestin, whereas undifferentiated UE7T-13 and H4-1 cells did not express mRNAs for Nurr1, NCAM, nestin, Sox-2, NF-M, or MAP-2 (Fig. 7), implying that these neuron-specific genes began to be expressed in response to the induction protocol (Fig. 5A). Sequence analysis confirmed that the PCR products matched the sequences of the human Nurr1, MAP2, tubulin 3, NF-M, NCAM, Notch-1, Sox-2, and nestin genes. Total brain mRNA was used as a positive control, and expression of all of the genes examined except the nestin gene was observed. The Notch-1 gene, a stem cell-related gene (18), is expressed only in undifferentiated cells and is absent in differentiated cells.

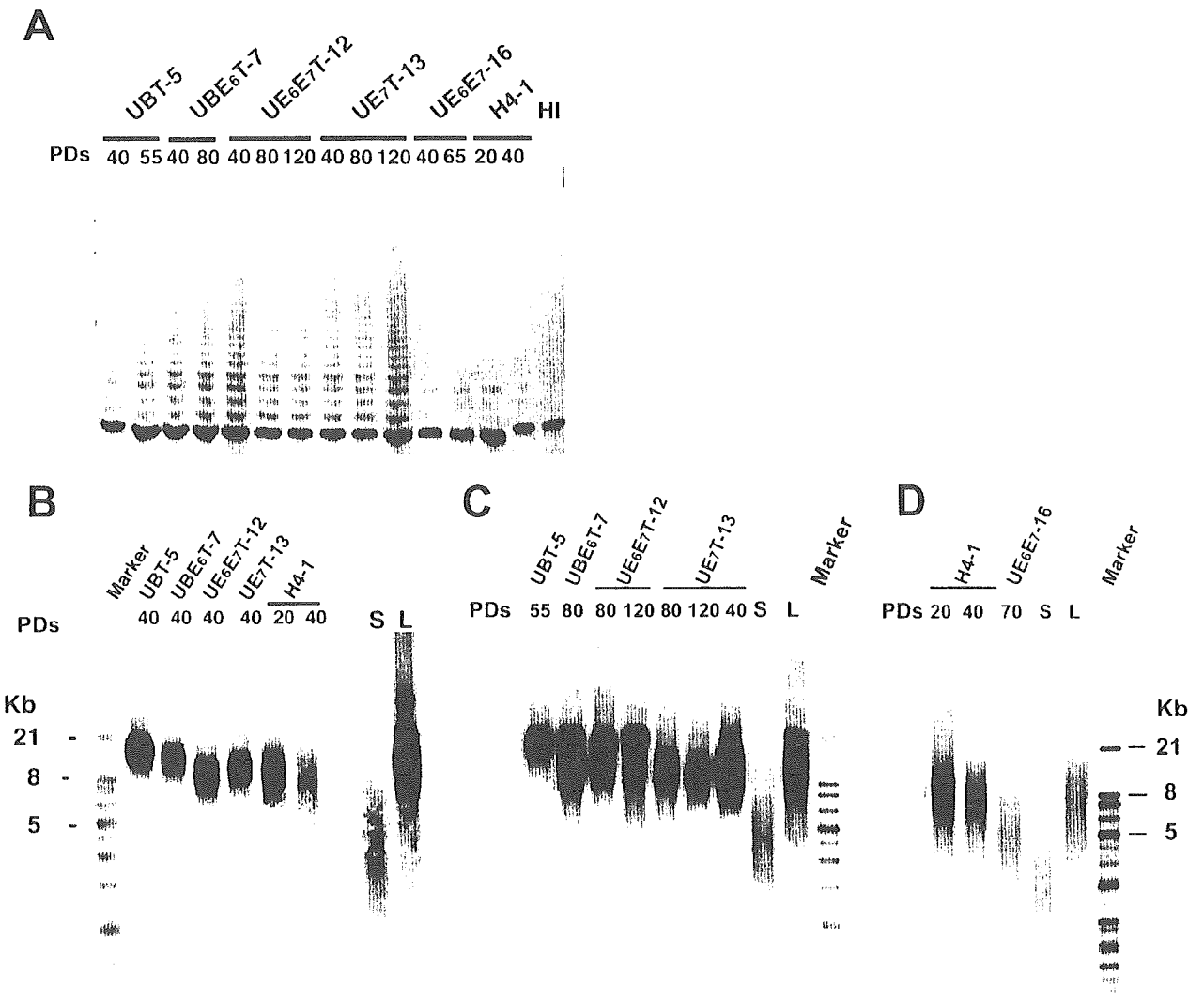

FIG. 3. Telomere activities and telomere lengths of the marrow stromal cells transduced with the hTERT and Bmi-1, E6, or E7 genes. (A) Analysis of telomerase activity by PCR assay in UBT-5, UBE6T-7, UE6E7T-12, UE7T-13, UE6E7-16, and H4-1 cells. Telomerase activity is revealed by the characteristic 6-bp ladder of bands. Heat-inactivated cell lysate (HI) was used as a negative control. (B, C, and D) The mean telomere length of the parental and transduced cells was determined at an early stage (B: 20 to 40 PDs) in UBT-5, UBE6T-7, UE6E7T-12, UE7T-13, and H4-1 cells; a late stage (C: 55 to 120 PDs) in UBT-5, UBE6T-7, UE6E7T-12, and UE7T-13 cells; and a senescent stage (D) in H4-1 and UE6E7-16 cells.

Tubulin 3 was detected at low levels in both differentiated and undifferentiated UE7T-13 cells.

Rapid and reversible calcium uptake by UE7T-13 cells in response to depolarizing stimuli. To determine if the neuronal cells derived from UE7T-13 cells are functional, we exposed the cells to depolarizing stimuli and performed calcium imaging analysis. Cells that had a dendrite component and a smooth-surfaced bright round soma body were selected as the targets for calcium-imaging analysis. Rapid and reversible calcium uptake was observed in neuronally differentiated UE7T-13 cells in response to the change in extracellular potassium concentration (Fig. 8), suggesting that the approximately 20% of the cells that showed uptake have both deep resting membrane potentials and voltage-gated Ca^{2+} channels. The rapid change in extracellular fluid did not cause any stretch-activated channels.

TABLE 1. Karyotypic analysis (G banding) in parental cells (H4-1) and clones

Cells	No. of PDs	No. of cells with indicated no. of chromosomes						
		44	45	46	47	48	49	50
H4-1	40	0	0	50	0	0	0	0
UBT-5	40	2	2	14	11	2	0	0
UBE6T-7	40	0	0	32	15	3	0	0
UE6E7T-12	40	0	1	45	2	0	0	0
UE7T-13	40	0	0	50	0	0	0	0
UE7T-13	80	0	0	50	0	0	0	0

Quantitative RT-PCR analysis of the *bmi-1*, TERT, E6, E7, and Nurr1 genes in UBT-5, UBE6T-7, UBE6E7T-12, and UE7T-13 cells with neuroectodermal induction at early and late PDs.

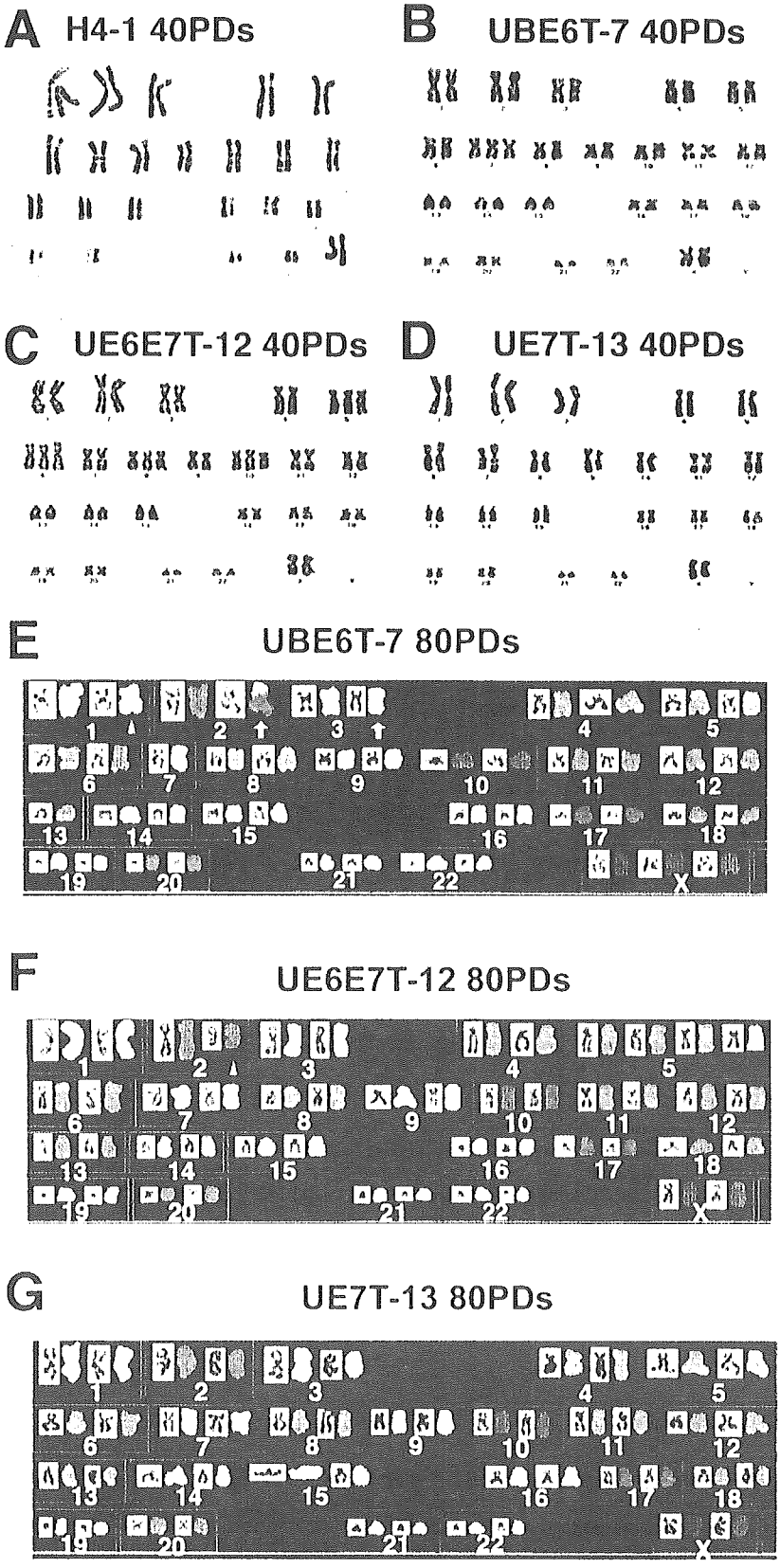

FIG. 4. Karyotypic analysis of parental and transduced cells with extended life spans. (A, B, C, and D) G-banded karyotyping. (E, F, and G) Spectral karyotyping. Metaphase spreads with structural chromosomal abnormalities were determined after the indicated number of PDs. Normal diploidy was seen in representative parental cells (A: H4-1) and UE7T-13 cells (B and G), but abnormalities were seen in UE6E7T-12 (C and F), UBE6T-7 (E), and UE7T-13 cells (D). Deletion and translocation are indicated by arrowheads and arrows, respectively.

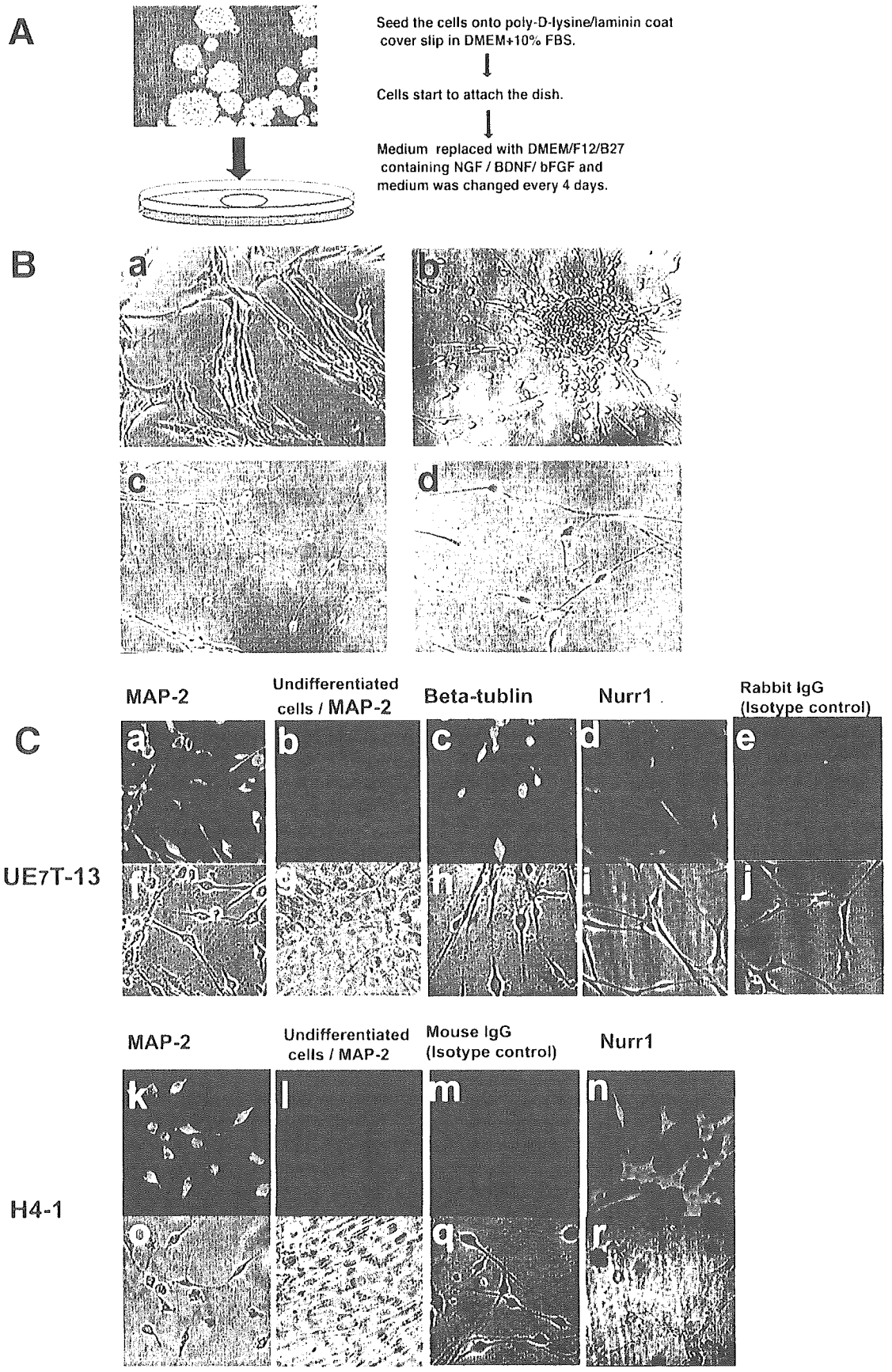
A
Seed the cells onto poly-D-lysine/laminin coat cover slip in DMEM+10% FBS.
Cells start to attach the dish.
Medium replaced with DMEM/F12/B27 containing NGF / BDNF/ bFGF and medium was changed every 4 days.
B
a
b
c
d
C
MAP-2
Undifferentiated cells / MAP-2
Beta-tublin
Nurr1
Rabbit IgG (Isotype control)
UE7T-13
MAP-2
Undifferentiated cells / MAP-2
Mouse IgG (Isotype control)
Nurr1
H4-1

TABLE 2. Genes regulated under neuronally differentiated conditions

Probe set	Description	Flag (N/C)[a]	Normalized value[b]	Fold change
Increased				
204621_s_at	Nurr1 (Nuclear receptor subfamily 4 group A member 2)	P/(A)	26.1	26.1
210663_s_at	Kynurenidase (L-kyurenine hydrolase)	P/(A)	60.7	9.6
204430_s_at	Solute carrier family 2 (facilitated glucose/fructose transporter), member 5	P/(A)	9.3	9.3
205921_s_at	Solute carrier family 6 (neurotransmitter transporter, taurine), member 6	P/(A)	6.2	6.2
205156_s_at	ACCN2 (amiloride-sensitive cation channel 2, neuronal)	P/(A)	4.1	3.4
204846_at	Ceruloplasmin (ferroxidase)	P/(A)	12.2	2.6
202507_s_at	Synaptosome-associated protein, 25 kDa	P/(A)	1.5	1.5
205792_at	WNT1-inducible signaling pathway protein 2	P/(P)	12.4	12.4
213425_s_at	WNT5A (wingless-type MMTV[c] integration site family, member 5A)	P/(P)	4.3	7.1
207594_s_at	Synaptojanin 1	P/(P)	3.3	6.1
211806_s_at	Potassium inwardly rectifying channel	P/(A)	2.5	2.5
211592_s_at	Calcium channel, voltage-dependent, L type	P/(A)	0.9	2.3
214933_at	Calcium channel, voltage-dependent, P/Q type	P/(A)	1.0	1.4
Decreased				
214081_at	Tumor endothelial marker 7	A/(P)	0.2	−19.5
209287_s_at	Cdc42 effector protein	A/(P)	0.1	−11.0
206898_at	Cadoherin 19, type 2	A/(P)	0.9	−7.1
205132_at	Actin alpha, cardiac muscle	A/(P)	0.1	−7.0
204736_s_at	Chondroitin 4-sulfotransferase	A/(P)	0.3	−5.0
209652_s_at	Placental growth factor, VEGF-related protein	A/(P)	1.0	−3.2
215177_s_at	Integrin alpha 6	A/(P)	0.5	−2.6

[a] N, neuronally differentiated UE7T-13 cells; C, undifferentiated UE7T-13 cells; P, judged to be "present" (expressed) in neuronally differentiated UE7T-13 cells; A, judged to be "absent" (not expressed) in undifferentiated UE7T-13 cells.

[b] The normalized values were calculated from data obtained in UE7T-13 cells as described in Material and Methods.

[c] MMTV, mouse mammary tumor virus.

We also performed an additional quantitative RT-PCR experiment to monitor the expression levels of the hTERT, *bmi-1*, E6, and E7 genes as well as the Nurr1 gene, during the neuronal differentiation of UBT-5, UBE6T-7, UE6E7T-12, and UE7T-13 cells (Table 3). The expression of the hTERT, E6, and E7 genes did not decrease and remained at a high level in neuronally differentiated cells. The *bmi-1* gene, on the other hand, was down-regulated. The Nurr-1 gene, a neuron marker, was significantly increased by neural induction, as expected. Although the hTERT, E6, and E7 genes were continuously strongly expressed during differentiation, the phenotype of the cells did not revert to an undifferentiated state and continued to exhibit neuronal phenotypes, even when bFGF, NGF, and BDNF were removed from the culture media.

DISCUSSION

Prolongation of the life span of human marrow stromal cells by *bmi-1*. This study was undertaken to investigate whether the life span of human marrow stromal cells, a candidate source of cells for therapy, can be prolonged by a cell-cycle associated molecule(s). Introduction of *bmi-1*, one of the polycomb group genes, clearly down-regulated p16, which is gradually induced as the number of PDs increases, and thus increases dephosphorylated Rb, resulting in the cell's escape from growth arrest or premature senescence, as we intended. This down-regulation of p16 is thought to be mediated via direct binding of *bmi-1* to the *cis*-regulatory element of p16, and thus the binding should be affected by the methylation status or chromatin structure of this *cis*-regulatory element. At the very least, *bmi-1* is functional in terms of decreasing p16 in human stromal cells, and the decrease in p16 leads to escape from premature senescence. This *bmi-1* effect on the cell life span has also been reported in human mammary epithelial cells (9), where it occurs via escape from replicative senescence by induction of telomerase activation; however, this effect of *bmi-1* on telomerase activation was not detected in our experimental human stromal cell system. In other words, *bmi-1* enables human stromal cells to escape from premature senescence but not replicative senescence.

The lack of change in phenotypes of *bmi-1*-transduced cells, for example, in their differentiation abilities, growth rates, cell surface markers, and gene expression profiles, is rather surprising, because *bmi-1* suppresses p16 protein and has been identified as a c-Myc-cooperating gene in murine B- and T-cell lymphomas (15, 37). A critical target of *bmi-1* is the *Ink4a* locus, which encodes p16 and p19 (p14 in humans) (14). In-

FIG. 5. Neuroectodermal differentiation of bone marrow stromal cells. (A) Scheme of the neuronal differentiation system. (B) Four phase-contrast microscopic images of UE7T-13 cells are shown. (a) Undifferentiated state. (b) Neuronally differentiated cells that had spread out to clusters. (c and d) Higher magnification of neuronally differentiated cells. (C) Fluorescence immunohistochemical analysis of undifferentiated UE7T-13 cells (b, g, l, and p) and neuronally differentiated cells (a, c to f, h to k, n to o, q, and r). (a, b, k, and l) MAP-2; (c) tubulin 3; (d and n) Nurr1. PE-conjugated anti-rabbit immunoglobulin G (IgG) (e) and fluorescein isothiocyanate-conjugated anti-mouse immunoglobulin antibody (m) were used as negative controls. (f, g, h, i, j, o, p, q, and r) Phase-contrast microscopic findings. All images were obtained with a laser scanning confocal microscope. (a to j) UE7T-13 cells; (k to r) H4-1 cells.

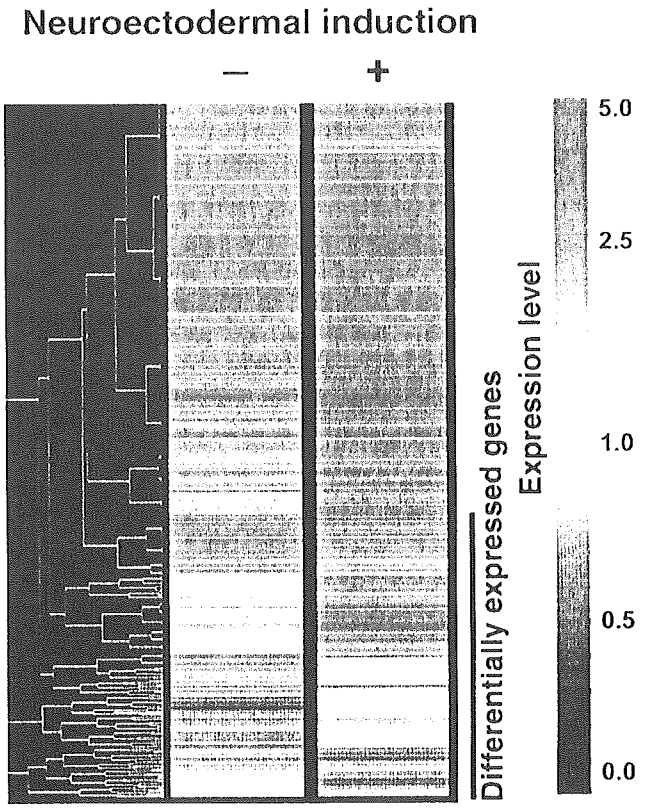

FIG. 6. Comparison between the gene profiles of neuroectodermal differentiated cells and undifferentiated cells. Gene expression levels in undifferentiated cells (−) and neuronally differentiated cells (+) are shown by the rows of colored bars that represent one gene. The color bars reflect the magnitude of the response for each gene according to the scale shown on the right. Differentially expressed genes are indicated by a vertical line on the right. The raw data from the gene chip analysis are available at the GEO database with accession number GSE2110 or our laboratory's website (http://1954.jukuin.keio.ac.jp/umezawa/chip/mori).

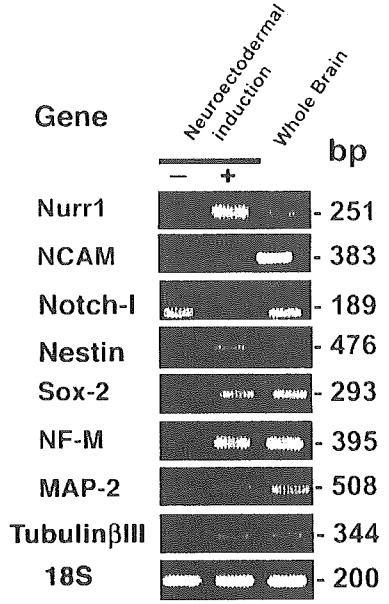

FIG. 7. RT-PCR analysis of expression of neuron-associated genes confirmed the gene chip data. RT-PCR analyses of RNAs from undifferentiated UE7T-13 cells, neuronally differentiated UE7T-13 cells, and human total brain were performed with primers that react with the human genes encoding MAP-2, tubulin 3, NF-M, Notch-1, NCAM, Sox-2, Nestin, and Nurr1. The signals of the 18S gene are approximately the same, indicating an equivalent input for all samples. Most of the neuron-associated genes were expressed by neuronally differentiated UE7T-13 cells and total brain cells.

terestingly, *bmi-1* is required for maintenance of adult self-renewing hematopoietic stem cells (29) and neural stem cells (25), whereas the simian virus 40 large T antigen oncogene, which prolongs the cell life span, interferes with the differentiation program and transforms cells. The human marrow-derived stromal cells transfected with simian virus 40 large T antigen (12) did not exhibit contact inhibition in vitro and formed tumors within a month when implanted into nude mice (data not shown).

Transdifferentiation of human mesoderm-derived cells into a functional neuronal lineage. This study was also conducted to determine whether prolongation of the cell life span by hTERT and *bmi-1*, E6, or E7 would predominate over neurogenic differentiation of marrow stromal cells in vitro. In contrast to our previous study of neurogenic differentiation of immortalized murine marrow-derived stromal cells (22) by demethylating agents, the transdifferentiation of the human stromal cells was limited to neurons, but not astrocytes or oligodendrocytes. This was probably due to the developmentally logical protocol we employed in this study: use of bFGF, NGF, BDNF, and laminin-ornithine coating. The idea for the neuronal differentiation protocol without 5-azacytidine arose from reports of the following: NGF and BDNF support neuron survival and growth (4), and bFGF induces initial differentiation of neural precursor cells and activates transcription factors related to the differentiation of neural precursor cells and embryonic stem cells (19, 31).

The extremely high level of expression of dopaminergic neuron-associated genes, such as *nurr1* and *wnt5a*, in the neuronally differentiated stromal cells, which we accidentally found by the GeneChip analysis and confirmed by RT-PCR, is surprising. *wnt5a* and *nurr1* are involved in the differentiation of midbrain precursors into dopaminergic neurons (20, 39). Although further analysis of functionally differentiated cells is beyond the scope of this study, it is quite interesting that dopaminergic neurons can be generated from marrow-derived stromal cells, since one of the target cells for regenerative medicine is dopaminergic neurons.

Are marrow stromal cells traced back to their default state, i.e., neural lineage, by neurotrophic factors? The mechanism of the transdifferentiation from marrow stromal cells to neuronal cells remains unresolved. It must be emphasized that the GeneChip analysis showed that the change in gene expression during differentiation is global and drastic: the differentiated cells no longer exhibited the profile of mesenchymal cells or the biphenotypic pattern of neuronal and mesenchymal cells. Contamination of human stromal cell cultures by neural precursor cells is inconceivable, because the cells were subcloned several times after gene transduction and exhibited mesenchymal phenotypes after subcloning. Our previous study of murine stromal cells clearly showed that osteoblasts capable of mem-

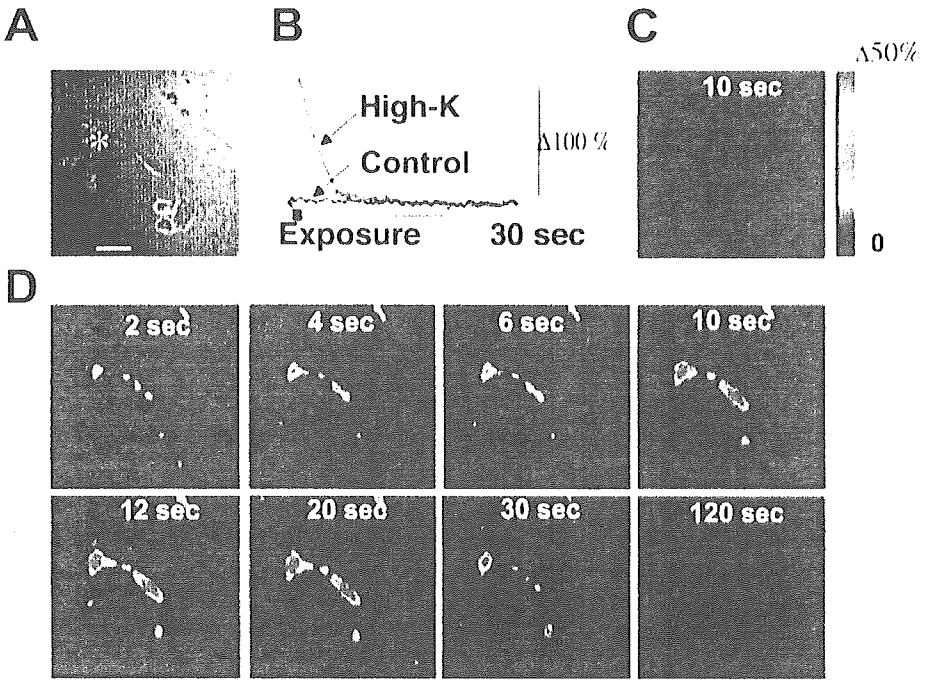

FIG. 8. Calcium imaging of neuronally differentiated stromal cells. (A) Phase-contrast photomicrograph of neuronally differentiated UE7T-13 cells. (B) The cell indicated by the asterisk in panel A showed rapid and reversible calcium uptake in response to high-potassium stimulation (red line; 115%), but simply changing the extracellular solution to the normal Tyrode's solution did not result in any calcium uptake (control; black line). Images obtained at 10 seconds after the high-potassium stimulation (D) and in the control (C). Rapid and reversible calcium uptake in response to high-potassium stimulation was observed in the four cells within this field.

TABLE 3. Quantitative RT-PCR analyses of the *bmi-1*, TERT, E6, E7, and Nurr1 genes in UBT-5, UBE6T-7, UBE6E7T-12, and UE7T-13 cells with neuroectodermal induction at early and late PDs

Cells/infected genes	No. of PDs	NI[a]	Expression level of genes[b]				
			bmi-1	TERT	E6	E7	Nurr1
UBT-5/Bmi1 and TERT	40	−	2.44	0.56			0.01
	75	−	2.13	0.48			0.02
	40	+	0.88	1.93			0.90
	75	+	0.73	6.47			1.17
UBE6T-7/*bmi-1*, E6, E7, and TERT	50	−	2.31	0.04	0.61		0.02
	120	−	0.55	0.29	0.21		0.02
	50	+	0.69	0.15	0.40		1.83
	120	+	0.15	1.18	0.87		2.69
UE6E7T-12/E6, E7, and TERT	33	−		0.35	0.62	0.28	0.02
	130	−		0.55	0.67	0.40	0.01
	33	+		0.62	4.05	1.49	2.91
	130	+		0.96	2.88	1.48	4.05
UE7T-13/E7 and TERT	33	−		0.63		1.22	0.01
	130	−		0.49		0.87	0.01
	33	+		1.17		1.01	0.78
	130	+		2.06		3.00	8.03

[a] NI, neuroectodermal induction; +, with NI; −, without NI.

[b] Cells removed from the flask bottom were placed on a coverslip coated with laminin-polylysin. One day after cell passage, the medium was replaced with B27-supplemented Dulbecco's modified Eagle's medium-F12 containing 20 ng/ml of BDNF, 10 ng/ml of bFGF, and 50 ng/ml of NGF to promote neuroectodermal differentiation. RNA was extracted from the cells for quantitative RT-PCR analysis 7 days after induction. The mRNA levels were normalized using the GAPDH gene as a housekeeping gene.

branous ossification are likely to differentiate into neuronal lineages but that adipocytes do not (22). The craniofacial membranous bones develop from the neural crest, which is of ectodermal origin. Our finding of in vitro differentiation from mesoderm- to ectoderm-derived cells in this study may be the opposite of the developmental process, i.e., from ectoderm- to mesoderm-derived cells. Development naturally progresses from neural crest cells to terminally differentiated osteoblasts (28). Converting differentiated osteoblasts or marrow stromal cells to neuronal cells, a key future task for any cell-based therapy, would thus oppose the usual direction of cell differentiation. This can now be achieved by exposing stromal cells to neurotrophic factors, at least in vitro.

Are human marrow stromal cells with an extended life span available for cell-based therapy? Human stromal cells transduced with hTERT and *bmi-1*, E6, or E7 did not transform according to the classical criteria: they did not generate tumors in immunosuppressed NOD-SCID-interleukin 2 receptor knockout mice, they did not form foci in vitro, and they stopped dividing after confluence (data not shown). However, we cannot rule out the possibility that gene-transduced stromal cells might become tumorigenic in patients several decades after cell therapy. We believe that these gene-modified stromal cells may be used to supply defective enzymes to patients with genetic metabolic diseases, such as neuro-Gaucher disease, Fabry disease, and mucopolysaccharidosis, which have a poor prognosis and are sometimes lethal. The "risk-versus-benefit" balance is essential when applying these gene-modified cells clinically, and the "risk" or "drawback" in this case is transformation of implanted cells.

hTERT is normally expressed in stem cells and in over 90% of human cancers. Ectopic expression of telomerase is sufficient to prevent telomere shortening and can thereby promote indefinite proliferation in human foreskin fibroblasts (5). Several stromal cell strains with extended life spans and maintenance of differentiation capability, such as UBT5, UBE6T7, UE6E7T-12, UE7T-13, and UE6E7-16 cells, were developed based on the above notion. UE6E7-16 cells not transduced with hTERT have a longer life span but enter a "crisis" period in culture at 67 PDs. "Crisis" is the stage in which widespread death occurs in a population of cultured cells or when karyotypic instability develops as a result of fusion of telomere ends, after the cells manage to circumvent senescence or initial blockades. Human cells transduced with *bmi-1* or E6 and E7 alone enter a "crisis," and the cells that spontaneously circumvent premature senescence without gene induction enter replicative senescence. Replicative senescence or crisis may be a tumor suppressor mechanism that avoids the risk of cell transformation after implantation of cells as a source for cell-based therapy.

Even when cells transduced with nononcogenic genes are used for cell-based therapy, the cases of leukemia in SCID patients treated with gene-modified lymphocytes must be taken into account (3). The infected virus genome was integrated into the LMO2 locus in the leukemia cases and resulted in induction of the oncogenic LMO2 gene. Because of these failures, it will take time before gene-modified cells can be used for regenerative medicine. Inhibition of the p16/Rb pathway is sufficient to prolong the life span of cells in cultures of marrow-derived stroma, as shown in this study. The p16/Rb pathway was activated in marrow-derived stromal cells in vitro, the same as in mammary epithelial cells and hepatocytes, but not in foreskin fibroblasts (21). The development of an appropriate culture system without gene transduction to neutralize the p16/Rb braking system, i.e., nonstress medium, will be essential for cell therapy and further experiments.

ACKNOWLEDGMENTS

We express our sincere thanks to K. Segawa, S. Matsumoto, Y. Okayama, S. Okuyama, and S. Ikeuchi for support throughout the work and to Y. Nakamura, N. Hida, N. Hashimoto, and T. Inomata for providing expert technical assistance. We are grateful to D. A. Galloway (FHCRC, Seattle, Wash.) for pLXSN-16E7 and to Y. Takeuchi (Chester Beatty Laboratories, ICR, United Kingdom) for the FLYA13 cells.

This work was supported in part by a special grant for Advanced Research on Cancer from the Ministry of Education, Culture, Sports, Science, and Technology (MEXT) of Japan to T.K. and A.U.; a grant from MEXT to A.U.; Health and Labour Sciences Research Grants to A.U.; and a grant from the Organization for Pharmaceutical Safety and Research to A.U.

REFERENCES

1. **Ahn, J. I., K. H. Lee, D. M. Shin, J. W. Shim, J. S. Lee, S. Y. Chang, Y. S. Lee, M. J. Brownstein, and S. H. Lee.** 2004. Comprehensive transcriptome analysis of differentiation of embryonic stem cells into midbrain and hindbrain neurons. Dev. Biol. **265**:491–501.
2. **Allan, E. H., P. W. Ho, A. Umezawa, J. Hata, F. Makishima, M. T. Gillespie, and T. J. Martin.** 2003. Differentiation potential of a mouse bone marrow stromal cell line. J. Cell Biochem. **90**:158–169.
3. **Allsopp, R. C., H. Vaziri, C. Patterson, S. Goldstein, E. V. Younglai, A. B. Futcher, C. W. Greider, and C. B. Harley.** 1992. Telomere length predicts replicative capacity of human fibroblasts. Proc. Natl. Acad. Sci. USA **89**: 10114–10118.
4. **Batchelor, P. E., G. T. Liberatore, M. J. Porritt, G. A. Donnan, and D. W. Howells.** 2000. Inhibition of brain-derived neurotrophic factor and glial cell line-derived neurotrophic factor expression reduces dopaminergic sprouting in the injured striatum. Eur. J. Neurosci. **12**:3462–3468.
5. **Bodnar, A. G., M. Ouellette, M. Frolkis, S. E. Holt, C. P. Chiu, G. B. Morin, C. B. Harley, J. W. Shay, S. Lichtsteiner, and W. E. Wright.** 1998. Extension of life-span by introduction of telomerase into normal human cells. Science **279**:349–352.
6. **Brazelton, T. R., F. M. Rossi, G. I. Keshet, and H. M. Blau.** 2000. From marrow to brain: expression of neuronal phenotypes in adult mice. Science **290**:1775–1779.
7. **Brewer, G. J., J. R. Torricelli, E. K. Evege, and P. J. Price.** 1993. Optimized survival of hippocampal neurons in B27-supplemented Neurobasal, a new serum-free medium combination. J. Neurosci. Res. **35**:567–576.
8. **Castelo-Branco, G., J. Wagner, F. J. Rodriguez, J. Kele, K. Sousa, N. Rawal, H. A. Pasolli, E. Fuchs, J. Kitajewski, and E. Arenas.** 2003. Differential regulation of midbrain dopaminergic neuron development by Wnt-1, Wnt-3a, and Wnt-5a. Proc. Natl. Acad. Sci. USA **100**:12747–12752.
9. **Dimri, G. P., J. L. Martinez, J. J. Jacobs, P. Keblusek, K. Itahana, M. Van Lohuizen, J. Campisi, D. E. Wazer, and V. Band.** 2002. The *bmi-1* oncogene induces telomerase activity and immortalizes human mammary epithelial cells. Cancer Res. **62**:4736–4745.
10. **Faux, C. H., A. M. Turnley, R. Epa, R. Cappai, and P. F. Bartlett.** 2001. Interactions between fibroblast growth factors and Notch regulate neuronal differentiation. J. Neurosci. **21**:5587–5596.
11. **Gojo, S., N. Gojo, Y. Takeda, T. Mori, H. Abe, S. Kyo, J. Hata, and A. Umezawa.** 2003. In vivo cardiovasculogenesis by direct injection of isolated adult mesenchymal stem cells. Exp. Cell Res. **288**:51–59.
12. **Hacein-Bey-Abina, S., C. Von Kalle, M. Schmidt, M. P. McCormack, N. Wulffraat, P. Leboulch, A. Lim, C. S. Osborne, R. Pawliuk, E. Morillon, R. Sorensen, A. Forster, P. Fraser, J. I. Cohen, G. de Saint Basile, I. Alexander, U. Wintergerst, T. Frebourg, A. Aurias, D. Stoppa-Lyonnet, S. Romana, I. Radford-Weiss, F. Gross, F. Valensi, E. Delabesse, E. Macintyre, F. Sigaux, J. Soulier, L. E. Leiva, M. Wissler, C. Prinz, T. H. Rabbitts, F. Le Deist, A. Fischer, and M. Cavazzana-Calvo.** 2003. LMO2-associated clonal T cell proliferation in two patients after gene therapy for SCID-X1. Science **302**: 415–419.
13. **Imabayashi, H., T. Mori, S. Gojo, T. Kiyono, T. Sugiyama, R. Irie, T. Isogai, J. Hata, Y. Toyama, and A. Umezawa.** 2003. Redifferentiation of dedifferentiated chondrocytes and chondrogenesis of human bone marrow stromal cells via chondrosphere formation with expression profiling by large-scale cDNA analysis. Exp. Cell Res. **288**:35–50.
14. **Jacobs, J. J., K. Kieboom, S. Marino, R. A. DePinho, and M. van Lohuizen.** 1999. The oncogene and Polycomb-group gene bmi-1 regulates cell proliferation and senescence through the ink4a locus. Nature **397**:164–168.
15. **Jacobs, J. J., B. Scheijen, J. W. Voncken, K. Kieboom, A. Berns, and M. van Lohuizen.** 1999. *bmi-1* collaborates with c-Myc in tumorigenesis by inhibiting c-Myc-induced apoptosis via INK4a/ARF. Genes Dev. **13**:2678–2690.
16. **Jiang, Y., D. Henderson, M. Blackstad, A. Chen, R. F. Miller, and C. M. Verfaillie.** 2003. Neuroectodermal differentiation from mouse multipotent adult progenitor cells. Proc. Natl. Acad. Sci. USA **100**(Suppl. 1):1854–1860.
17. **Kageyama, R., and T. Ohtsuka.** 1999. The Notch-Hes pathway in mammalian neural development. Cell Res. **9**:179–188.
18. **Kageyama, R., T. Ohtsuka, and K. Tomita.** 2000. The bHLH gene Hes1 regulates differentiation of multiple cell types. Mol. Cell **10**:1–7.
19. **Kalyani, A. J., T. Mujtaba, and M. S. Rao.** 1999. Expression of EGF receptor and FGF receptor isoforms during neuroepithelial stem cell differentiation. J. Neurobiol. **38**:207–224.
20. **Kim, J. H., J. M. Auerbach, J. A. Rodriguez-Gomez, I. Velasco, D. Gavin, N. Lumelsky, S. H. Lee, J. Nguyen, R. Sanchez-Pernaute, K. Bankiewicz, and R. McKay.** 2002. Dopamine neurons derived from embryonic stem cells function in an animal model of Parkinson's disease. Nature **418**:50–56.
21. **Kiyono, T., S. A. Foster, J. I. Koop, J. K. McDougall, D. A. Galloway, and A. J. Klingelhutz.** 1998. Both Rb/p16INK4a inactivation and telomerase activity are required to immortalize human epithelial cells. Nature **396**:84–88.
22. **Kohyama, J., H. Abe, T. Shimazaki, A. Koizumi, K. Nakashima, S. Gojo, T. Taga, H. Okano, J. Hata, and A. Umezawa.** 2001. Brain from bone: efficient "meta-differentiation" of marrow stroma-derived mature osteoblasts to neurons with Noggin or a demethylating agent. Differentiation **68**:235–244.
23. **Le, W. D., P. Xu, J. Jankovic, H. Jiang, S. H. Appel, R. G. Smith, and D. K. Vassilatis.** 2003. Mutations in NR4A2 associated with familial Parkinson disease. Nat. Genet. **33**:85–89.
24. **Makino, S., K. Fukuda, S. Miyoshi, F. Konishi, H. Kodama, J. Pan, M. Sano, T. Takahashi, S. Hori, H. Abe, J. Hata, A. Umezawa, and S. Ogawa.** 1999. Cardiomyocytes can be generated from marrow stromal cells in vitro. J. Clin. Investig. **103**:697–705.
25. **Molofsky, A. V., R. Pardal, T. Iwashita, I. K. Park, M. F. Clarke, and S. J. Morrison.** 2003. *bmi-1* dependence distinguishes neural stem cell self-renewal from progenitor proliferation. Nature **425**:962–967.
26. **Ochi, K., G. Chen, T. Ushida, S. Gojo, K. Segawa, H. Tai, K. Ueno, H. Ohkawa, T. Mori, A. Yamaguchi, Y. Toyama, J. Hata, and A. Umezawa.** 2003. Use of isolated mature osteoblasts in abundance acts as desired-shaped

bone regeneration in combination with a modified poly-DL-lactic-co-glycolic acid (PLGA)-collagen sponge. J. Cell Physiol. **194**:45–53.
27. **Okamoto, T., T. Aoyama, T. Nakayama, T. Nakamata, T. Hosaka, K. Nishijo, T. Nakamura, T. Kiyono, and J. Toguchida.** 2002. Clonal heterogeneity in differentiation potential of immortalized human mesenchymal stem cells. Biochem. Biophys. Res. Commun. **295**:354–361.
28. **Olsen, B. R., A. M. Reginato, and W. Wang.** 2000. Bone development. Annu. Rev. Cell Dev. Biol. **16**:191–220.
29. **Park, I. K., D. Qian, M. Kiel, M. W. Becker, M. Pihalja, I. L. Weissman, S. J. Morrison, and M. F. Clarke.** 2003. *bmi-1* is required for maintenance of adult self-renewing haematopoietic stem cells. Nature **423**:302–305.
30. **Sano, M., A. Umezawa, H. Abe, A. Akatsuka, S. Nonaka, H. Shimizu, M. Fukuma, and J. Hata.** 2001. EAT/mcl-1 expression in the human embryonal carcinoma cells undergoing differentiation or apoptosis. Exp. Cell Res. **266**: 114–125.
31. **Santa-Olalla, J., and L. Covarrubias.** 1995. Epidermal growth factor (EGF), transforming growth factor-alpha (TGF-alpha), and basic fibroblast growth factor (bFGF) differentially influence neural precursor cells of mouse embryonic mesencephalon. J. Neurosci. Res. **42**:172–183.
32. **Satoh, J., and Y. Kuroda.** 2002. The constitutive and inducible expression of Nurr1, a key regulator of dopaminergic neuronal differentiation, in human neural and non-neural cell lines. Neuropathology **22**:219–232.
33. **Scheffner, M., K. Munger, J. M. Huibregtse, and P. M. Howley.** 1992. Targeted degradation of the retinoblastoma protein by human papillomavirus E7-E6 fusion proteins. EMBO J. **11**:2425–2431.
34. **Schrock, E., T. Veldman, H. Padilla-Nash, Y. Ning, J. Spurbeck, S. Jalal, L. G. Shaffer, P. Papenhausen, C. Kozma, M. C. Phelan, E. Kjeldsen, S. A. Schonberg, P. O'Brien, L. Biesecker, S. du Manoir, and T. Ried.** 1997. Spectral karyotyping refines cytogenetic diagnostics of constitutional chromosomal abnormalities. Hum. Genet. **101**:255–262.
35. **Sekiguchi, T., and T. Hunter.** 1998. Induction of growth arrest and cell death by overexpression of the cyclin-Cdk inhibitor p21 in hamster BHK21 cells. Oncogene **16**:369–380.
36. **Terai, M., T. Uyama, T. Sugiki, X. K. Li, A. Umezawa, and T. Kiyono.** 2005. Immortalization of human fetal cells: the life span of umbilical cord blood-derived cells can be prolonged without manipulating p16INK4a/RB braking pathway. Mol. Biol. Cell **16**:1491–1499.
37. **van Lohuizen, M., S. Verbeek, B. Scheijen, E. Wientjens, H. van der Gulden, and A. Berns.** 1991. Identification of cooperating oncogenes in E mu-myc transgenic mice by provirus tagging. Cell **65**:737–752.
38. **Wright, W. E., and J. W. Shay.** 1992. The two-stage mechanism controlling cellular senescence and immortalization. Exp. Gerontol. **27**:383–389.
39. **Zetterstrom, R. H., L. Solomin, L. Jansson, B. J. Hoffer, L. Olson, and T. Perlmann.** 1997. Dopamine neuron agenesis in Nurr1-deficient mice. Science **276**:248–250.

Available online at www.sciencedirect.com
SCIENCE DIRECT®
Biochemical and Biophysical Research Communications 332 (2005) 1004–1011
BBRC
www.elsevier.com/locate/ybbrc

Laminin binding protein, 34/67 laminin receptor, carries stage-specific embryonic antigen-4 epitope defined by monoclonal antibody Raft.2

Yohko U. Katagiri [a,b,*], Nobutaka Kiyokawa [a], Kyoko Nakamura [c], Hisami Takenouchi [a], Tomoko Taguchi [a], Hajime Okita [a], Akihiro Umezawa [d], Junichiro Fujimoto [a]

[a] *Department of Developmental Biology, National Research Institute for Child Health and Development, Setagaya-ku, Tokyo 157-8535, Japan*
[b] *Japan Science and Technology Corporation, CREST, Japan*
[c] *Supra-Biomolecular System Research Group, RIKEN Frontier System Research, Wako-shi, Saitama 351-0198, Japan*
[d] *Department of Reproductive Biology, National Research Institute for Child Health and Development, Setagaya-ku, Tokyo 157-8535, Japan*

Received 24 April 2005
Available online 23 May 2005

Abstract

We previously produced monoclonal antibodies against the detergent-insoluble microdomain, i.e., the raft microdomain, of the human renal cancer cell line ACHN. Raft.2, one of these monoclonal antibodies, recognizes sialosyl globopentaosylceramide, which has the stage-specific embryonic antigen (SSEA)-4 epitope. Although the mouse embryonal carcinoma (EC) cell line F9 does not express SSEA-4, some F9 cells stained with Raft.2. Western analysis and matrix-assisted laser desorption ionization-time of flight mass spectrometry identified the Raft.2 binding molecule as laminin binding protein (LBP), i.e., 34/67 laminin receptor. Weak acid treatment or digestion with *Clostridium perfringens* sialidase reduced Raft.2 binding to LBP on nitrocellulose sheets and [^{14}C]galactose was incorporated into LBP, indicating LBP to have a sialylated carbohydrate moiety. Subcellular localization analysis by sucrose density-gradient centrifugation and examination by confocal microscopy revealed LBP to be localized on the outer surface of the plasma membrane. An SSEA-4-positive human EC cell line, NCR-G3 cells, also expressed Raft.2-binding LBP.

Keywords: SSEA-4; SialylGb5; Embryonal carcinoma; Laminin binding protein; Laminin receptor; Raft.2; MALDI-TOF MS

EC derived from testicular teratocarcinomas are a subset of germ cell tumors that may contain many embryonic and extra-embryonic tissues, and they represent malignant replicas of normal embryonic cells at specific stages of development. Immunochemical markers, such as SSEA-1, -3, and -4, TRA-1-60, and TRA-1-81, have been utilized to characterize and define the developmental stages of EC lines. For example, early cleavage-stage mouse embryos [1] and the primitive and visceral yolk sac endodermal cells of post-implantation mouse embryos [2] express SSEA-3 and SSEA-4. These carbohydrate antigens are also found on human, but not on murine, EC cells [3]. By contrast, murine EC cells express SSEA-1, while human EC cells do not. Exposure to retinoic acid can prompt EC cells to develop to advanced stages, accompanied by changes in SSEA expressions. Many monoclonal antibodies defining SSEAs were generated in early studies of mammalian development. SSEA-1 is an antigenic epitope defined as a Lewis x (Le^x) carbohydrate structure and is found in both glycosphingolipids and glycoproteins [1,4]. SSEA-3 and -4 defined by MC631 and MC813-70, respectively,

* Corresponding author. Fax: +81 3 3487 9669.
E-mail address: kata@nch.go.jp (Y.U. Katagiri).

0006-291X/$ - see front matter © 2005 Elsevier Inc. All rights reserved.
doi:10.1016/j.bbrc.2005.05.052

are located in carbohydrate moieties of globoseries glycosphingolipids [5].

We previously established a monoclonal antibody (Mab) termed Raft.2 by subcutaneously injecting the raft microdomain of a human renal cancer cell line, ACHN, into Balb/c mice and showed that Raft.2 recognizes the carbohydrate structure of sialosyl globopentaosylceramide (sialylGb5), namely GL7, the epitope of SSEA-4 [6]. SSEAs are still among the best markers for characterizing embryonic stem (ES) cells or EC cells and Raft.2 is a potentially useful tool for this purpose.

Although mouse EC F9 cells are known to be SSEA-4 negative, some of these cells stained with Raft.2. In this study, we demonstrated that Raft.2 binds to LBP and that Raft.2-positive LBP is present not only in F9 cells, but also in human EC NCR-G3 cells. We also show LBP to be localized on surface membranes and discuss the significance of LBP carrying SSEA-4. This is the first report, to our knowledge, focusing the SSEA-4 carried by LBP.

Materials and methods

Cell culture and antibodies. The mouse EC cell line F9 and the human renal cancer cell line ACHN were purchased from the American Type Culture Collection. F9 cells were cultured in Dulbecco's modified Eagle's medium (DMEM) (Sigma Chem., St. Louis, MO) supplemented with 10% fetal bovine serum (Sigma). ACHN was cultured in Eagle's minimum essential medium (MEM) (Sigma) supplemented with 10% fetal bovine serum and the non-essential amino acid solution (Sigma). The human EC cell line, NCR-G3 [7], was cultured in a 1:1 mixture of DMEM and Ham's F12 medium (Gibco, Grand Island, NY) supplemented with 10% fetal bovine serum, insulin–transferrin–sodium selenite media (Sigma), and the non-essential amino acid solution. MC-631, Mab for SSEA-3 and MC-813-70, Mab for SSEA–4, to detect Gb5 and sialylGb5, respectively, were purchased from Chemicon International (Temecula, CA). 13C4, Mab for Shiga toxin 1-B subunit (Stx1B), and T-20, a rabbit anti-mouse GTP binding protein β subunit (Gβ) polyclonal antibody, were purchased from the American Type Culture Collection and Santa Cruz Biotechnology (Santa Cruz, CA), respectively.

Glycolipid analysis. The packed cell pellet (0.5 ml) was extracted with 2 ml chloroform/methanol (C/M) (2:1, v/v) and then with 2 ml of chloroform/isopropanol/water (7:11:2, v/v). Total extracts were combined and evaporated to dryness and then treated with 0.2 N KOH in methanol at 37 °C for 2 h to saponify the phospholipids. After neutralization, methyl esters of fatty acids were removed by mixing with hexane. The extracts were then concentrated to 1/10 volume and dialyzed against water. The retentate was freeze-dried and dissolved in C/M (2:1).

Thin layer chromatography (TLC) immunostaining was performed according to a previously described method [8]. Briefly, C/M extracts were separated on plates precoated with Silica gel 60 (HPTLC aluminium sheets, Merck, Darmstadt Germany) using a solvent system consisting of C/M/water containing 0.1% $CaCl_2$ (5:4:1, v/v/v). After drying, the plates were dipped in 0.1% polyisobutylmethacrylate (Aldrich Chem., Milwaukee, WI, USA) in cyclohexane for 1 min and blocked with 1% bovine serum albumin (BSA) in phosphate-buffered saline (PBS). The plates were probed with Shiga toxin 1-B subunit (Stx1B) (1 μg/ml in 1% BSA) [9], then Mab 13C4 culture supernatant to detect globotriaosylceramide (Gb3), and with Mab Raft.2 culture supernatant to detect sialylGb5. After three washes with PBS for 5 min each, horseradish peroxidase-conjugated rabbit anti-mouse immunoglobulins (DAKO, A/S, Denmark) at a 1:2000 dilution ratio were used as the second antibody. The antibodies that bound to the plates were visualized with enhanced chemiluminescence reagent SuperSignal (Pierce, Rockford, IL, USA) and detected by LAS-1000 (Fuji Film, Tokyo, Japan).

Flowcytometry. Cells were harvested and incubated with a 1st antibody for 1 h on ice, followed by treatment with fluorescein isothiocyanate-conjugated goat anti-mouse immunoglobulins (Jackson Laboratory, West Grove, PA) at a 1:50 dilution ratio and analyzed by flowcytometry (EPICS-XL, Beckman–Coulter).

Western analysis. Cells were homogenized in hypotonic buffer (25 mM NaCl, 0.5 mM $CaCl_2$, 18 mM Tris–HCl buffer, pH 8.0) and cell debris was removed by centrifugation at 200*g* for 5 min at 4 °C. Precipitates were homogenized in the same manner two more times. The combined supernatants were centrifuged at 40K rpm for 30 min at 4 °C in a Beckman 80Ti rotor to obtain crude membrane fractions. The membrane proteins released with 1% Triton X-100 in 25 mM Tris–HCl buffer, pH 7.5, containing 0.15 M NaCl and the cocktail of protease inhibitors, were subjected to 1-dimensional (1-D) or 2-D Western analysis as previously described [10]. In order to remove the sialic acids from the glycoproteins, after 1-D Western blotting, the membrane strips were treated with 25 mM H_2SO_4 at 80 °C for 1 h.

Matrix-assisted laser desorption ionization-time of flight mass spectrometry (MALDI-TOF MS) analysis. The membrane proteins were separated by 2-D polyacrylamide gel electrophoresis (PAGE) and stained with Coomassie brilliant blue (CBB) R-250 (Bio-Rad Lab., Richmond, CA). The CBB-stained protein that corresponded to the position of the Raft.2-reacting spot was excised and digested with trypsin, and the trypsinized peptides were analyzed with an oMALDI-Qq-TOF MS/MS QSTAR Pulser *i* (Applied Biosystems). The mass spectra search was conducted using an NCBI non-reductant database with the MASCOT search algorithm.

Metabolic labeling of F9 cells with [^{14}C]galactose. Subconfluent cells (approx. 1.4×10^6 cells) were cultured in 4 ml of the incubation medium containing 10 μCi D-[1-^{14}C]galactose (57 mCi/mmol, 200 μCi/ml, Amersham Biosciences UK) for 24 h in a 60 mm culture plate. [^{14}C]Galactose-labeled membrane protein was prepared as above and mixed with 50 μg of non-labeled F9 membrane proteins. The F9 membrane protein mixture thus obtained was separated by 2-D PAGE and stained with CBB. Autoradiograms were obtained with BAS 2000.

Sialidase treatment. Proteins on 2-D nitrocellulose sheets were stained with Ponceau 3R Stain Solution (Wako Pure Chem., Osaka, Japan) and the rectangle containing the proteins of interest was excised. The blots were incubated in 50 mM sodium acetate buffer, pH 4.5, containing 0.1% BSA, with or without 100 mU of neuraminidase from *Clostridium perfringens* (Roche Diagnosis GmbH, Mannheim, Germany) at 37 °C overnight.

Subcellular fractionation. Crude membrane fractions obtained as described above were thoroughly suspended in the hypotonic buffer containing 30% sucrose and overlaid on a discontinuous sucrose density gradient of 40%/45%/50%/60% in a 12-ml ultracentrifugation tube, and the suspension was then overlaid with a 20% sucrose layer. The gradient was centrifuged at 25K rpm for 1 h in a Beckman SW40Ti rotor, and after recovery and dilution with PBS, each of the interface layers was sedimented at 40K rpm for 0.5 h in a Beckman 80Ti rotor. Proteins were released from each precipitate with 1% Triton X-100 lysis buffer and subjected to 2-D PAGE.

Staining for fluorescence microscopic observation. EC cells were harvested from cell culture plates and incubated with Raft.2. They were then stained with Alexa Fluor 488-conjugated goat anti-mouse IgM, μ-chain (Molecular probes, Eugene, OR) for 1 h and mounted in Perma Fluor Aqueous Mounting Medium (Thermo Shandon, Pittsburgh, PA) on a slide glass. The slides were observed with an Olympus LSM-GB200 confocal microscope.

Results

The sialylGb5 expressions on murine and human EC cells were examined by TLC immunostaining and flowcytometry with two Mabs against SSEA-4, Raft.2, and MC-813-70. ACHN cells, which express globoseries glycolipids, such as Gb3 and sialylGb5, were also examined and compared, as a control. All of these cell lines synthesized Gb3 (Fig. 1A, left panel). SialylGb5 was synthesized by ACHN and NCR-G3, but not F9, cells (Fig. 1A, right panel). ACHN and NCR-G3 cells were confirmed to express both sialylGb5 and Gb5 on their surface by flowcytometry (Fig. 1B, upper and lower row). Flowcytometric analysis further confirmed SSEA-4 expression on small populations (8.42%+) of F9 cells using Raft.2 and the faint expression using MC-813-70 (Fig. 1B, middle row). The staining profile of MC-631 was similar to that of Raft.2 (6.7%+). Taking these observations together, although F9 cells do not synthesize sialylGb5, they clearly express the SSEA-4 epitope on their surfaces.

We performed Western analysis to ascertain whether the SSEA-4-carried molecules are glycoproteins. Cytoplasmic proteins and 1% Triton membrane lysates of F9 cells were subjected to 1-D and 2-D Western analysis. Mab Raft.2 definitely bound to a membrane protein with an apparent molecular weight (mw) of 44K (Fig. 2A), but did not bind to cytoplasmic proteins (data not shown). Since Raft.2 cannot bind to Gb5, sialic acid residue is prerequisite for Raft.2 binding to the SSEA-4 epitope. Weak acid treatment of the blot markedly diminished Raft.2 binding to the 44K protein, while only minimally decreasing T-20 binding to its antigen, Gβ. These findings indicate that the carbohydrate chain of the protein is sialylated. 2-D Western analysis yielded

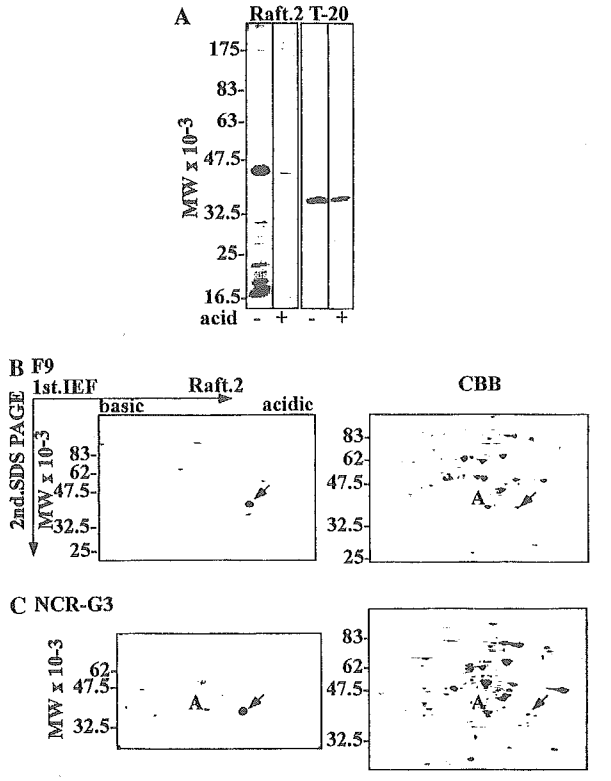

Fig. 2. Western analysis of the Raft.2 binding protein. (A) Membrane proteins of F9 cells were separated to four lanes by 1-D SDS–PAGE and transferred to a nitrocellulose sheet. Two of the strips were treated with weak acid (+), the other two were not (−). Two (− and +) were probed with Raft.2 (left), the other two with T-20 (right). (B) The membrane proteins separated by 2-D PAGE were transferred to a nitrocellulose sheet and probed with Raft.2 (left panel) or the membrane proteins in a 2-D gel were stained with CBB (right panel). The arrow points to the spot bound by Raft.2 and "A" indicates actin. (C) Membrane proteins of NCR-G3 cells were analyzed as in (B).

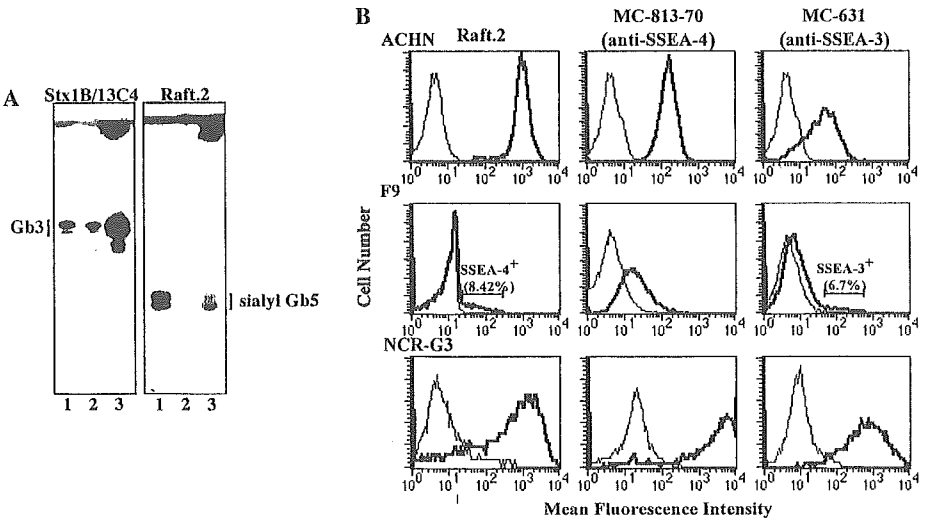

Fig. 1. Expression of SSEA-4 by the murine and human EC cell lines, F9 cells, and NCR-G3. (A) Total lipids from ACHN cells (lane 1), F9 cells (lane 2), and NCR-G3 cells (lane 3) were separated by TLC and immunostained with Stx1B/13C4 (left) and Raft.2 (right). (B) Cells were stained with Raft.2 (left row), MC-813-70 (middle row), or MC-631 (right row) and with a FITC-conjugate secondary antibody and analyzed by flowcytometry.

a single spot at an isoelectric point (p*I*) of 5.0 (Fig. 2B, left panel), slightly more acidic than actin (Fig. 2B, right panel). NCR-G3 cells expressed exactly the same Raft.2-positive proteins as F9 cells (Fig. 2C). The other two anti-SSEA Mabs, MC-813-70 and MC-631, bound none of the SDS-denatured proteins on a nitrocellulose sheet (data not shown).

In order to identify the spot bound by Mab Raft.2, we carried out MALDI-TOF MS/MS analysis of this spot in a 2-D gel (Fig. 2B). Eleven possible peptide signals with masses (*m/z*) of 912.6, 1200, 1203.6, 1291.7, 1419.8, 1615, 1698, 1740.9, 2082.1, 2172.2, and 2298.2, respectively, were detected (Fig. 3, underlined) and matched to the fragments of 40S ribosomal protein SA, known as 34/67 laminin receptor or LBP. The MS/MS spectra of five peptides (*) were obtained and the fragments were matched to the sequence from Lys_{42} to Arg_{128} of LBP (Table 1).

In order to confirm that LBP has a sialylated carbohydrate chain, we examined whether [^{14}C]galactose is incorporated into LBP. Membrane proteins prepared from F9 cells, which were metabolically labeled with [^{14}C]galactose, were separated by 2-D PAGE and subjected to autoradiography. The LBP spot was detected on the autoradiogram obtained by BAS 2000 (Fig. 4A). Next, we examined the effect of sialidase digestion on Raft.2 binding. Two nitrocellulose sheets, on which membrane proteins of NCR-G3 cells had been separated by 2-D PAGE followed by transfer, were stained with Ponceau 3R Stain (Fig. 4B). Small rectangles containing LBP were excised from the nitrocellulose sheets. The excised blot was incubated in 50 mM sodium acetate buffer, pH 4.5, with or without *C. perfringens* sialidase to release terminal sialic acids from glycoconjugates. This treatment reduced the Raft.2 binding to LBP (Fig. 4C), confirming that LBP contains sialic acid.

Table 1
Mass fragments fitted for murine LBP by Mascot search

m/z	Start	End	Peptide sequence
912.6*	121	128	LLVVTDPR
1200	54	63	TWEKLLLAAR
1203.6*	90	102	FAAATGATPIAGR
1291.7	43	53	SDGIYIINLKR
1419.8	42	53	KSDGIYIINLKR
1615*	86	102	AVLKFAAATGATPIAGR
1698	103	117	FTPGTFTNQIQAAFR
1740.9*	64	80	AIVAIENPADVSVISSR
2082.1*	103	120	FTPGTFTNQIQAAFREPR
2172.2	81	102	NTGORAVLKFAAATGATPIAGR

The five fragments (*) were subjected to MS/MS analysis.

Next, we fractionated the organelles of F9 cells by sucrose density gradient centrifugation to identify the

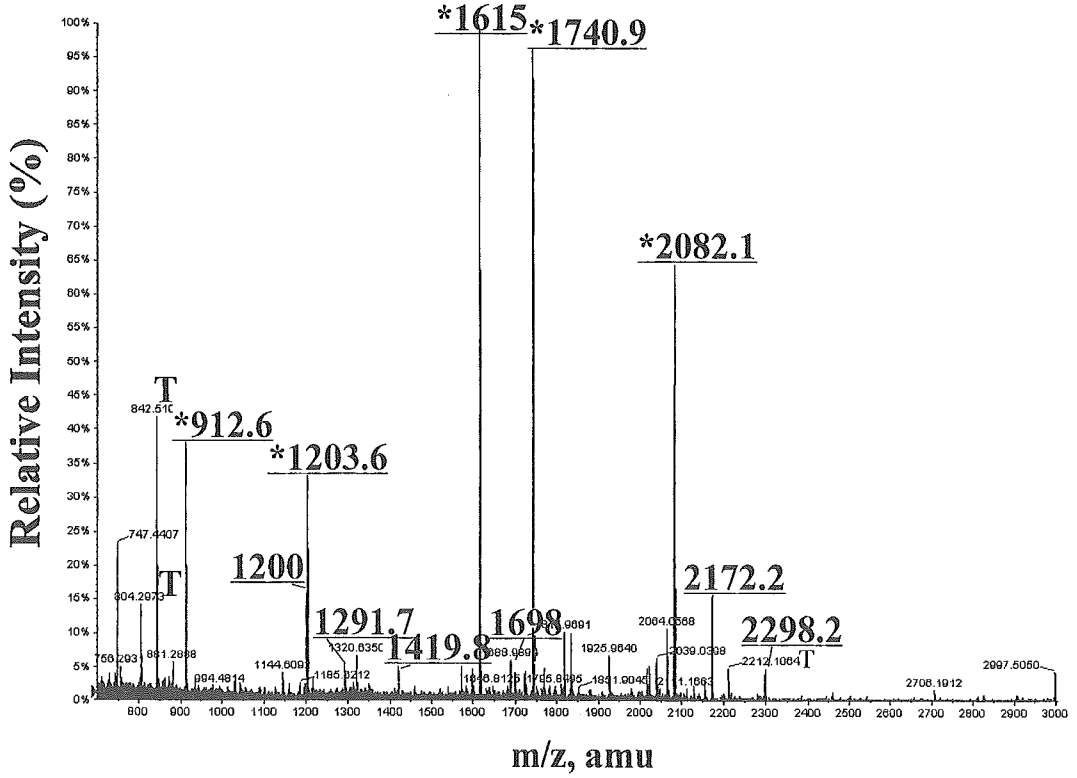

Fig. 3. MALDI-TOF MS spectra of the mw 44K molecule recognized by Raft.2. The Raft.2-binding molecule indicated by the arrow in Fig. 2C was in-gel digested with trypsin and subjected to oMALDI-Qq-TOF MS/MS QSTAR Pulser *i* spectrometry. The masses of the underlined peaks matched those of LBP. The peaks marked "T" were derived from trypsin.

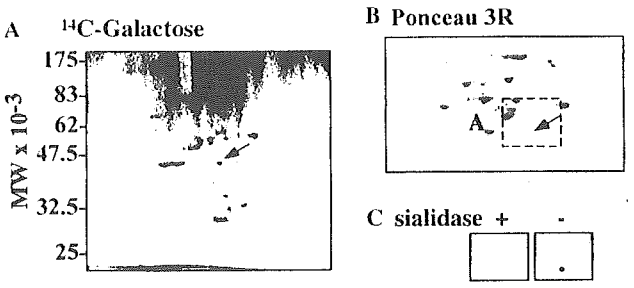

Fig. 4. Detection of galactose and sialic acid residues in LBP. (A) Autoradiogram of membrane proteins prepared from [^{14}C]galactose-labeled F9 cells and separated by 2-D PAGE. (B) The membrane proteins separated by 2-D PAGE were transferred to a nitrocellulose sheet and stained with Ponceau 3R. "A" indicates actin and the arrows point to LBP. (C) The blot containing LBP was incubated with (+) and without (−) sialidase and probed with Raft.2.

organelles in which LBP was localized. Triton X-100 lysates of each layer were 2-D separated and stained with CBB (Fig. 5). Since Src kinase Yes was found only in layer 1 (data not shown), the plasma membrane appears to be recovered from layer 1. Nuclear fragments were precipitated to the bottom. LBP was found only in layer 1, indicating that LBP is localized in plasma membranes.

fsConfocal microscopic observation confirmed Raft.2 binding on the cell surface. Cell suspensions of F9 and NCR-G3 were stained with Raft.2 and observed with a confocal microscope. Since Raft.1 recognizes Gβ located within cells [10], no F9 cells were stained with Raft.1 (Fig. 6A). As shown in Fig. 6B, some cells showed uneven, dot-like staining with Raft.2, while others did not. This indicates that some, not all, F9 cells express Raft.2 binding molecules on their cell surfaces. NCR-G3 cells were evenly stained with Raft.2 (Fig. 6C).

Discussion

We previously established Mab Raft.2, which specifically binds to sialylGb5 on TLC and cell surfaces. SialylGb5 carries the SSEA-4 epitope, which is naturally found in glycolipids. Interestingly, although mouse EC cell line F9 cells do not express sialylGb5, they are stained with Raft.2. Western analysis and the subsequent mass spectrometric analysis revealed the Raft.2 binding molecule to be LBP. The human EC cell line NCR-G3, which synthesizes sialylGb5, was also found to express Raft.2-binding LBP. Weak acid treatment or sialidase digestion reduced Raft.2 binding to LBP and [^{14}C]galactose was incorporated into LBP. These results confirm that LBP carries the SSEA-4 epitope. The precise carbohydrate structure of LBP must be obtained to provide further confirmation. Mass spectrometric analysis of the sugar moiety of LBP is currently underway, employing microLC-ESI MS/MS.

Raft.2 is different from another anti-SSEA-4 Mab, MC-813-70 in reactivity with SSEA-4 epitope. Raft.2 did not react with GM1b purified from mouse spleen [11] (data not shown), but MP-813-70 does [5]. These two Mabs appear to be different from each other in reactivity with glycoproteins.

Many developmentally regulated antigens, including SSEAs, ABH, Forssman, globoside, and Ii, are carbohydrates in nature [12]. Such antigenic determinants are carried by lipids and/or by protein molecules. It was previously reported that SSEA-1, i.e., Lewis x antigen (Le^x), is carried by both proteins [13] and lipids [4] and that SSEA-3 is carried by both membrane glycolipids and glycoproteins [1]. By contrast, it is generally accepted that the SSEA-4 is carried only by globoseries glycosphingolipids [5]. Herein, however, we present

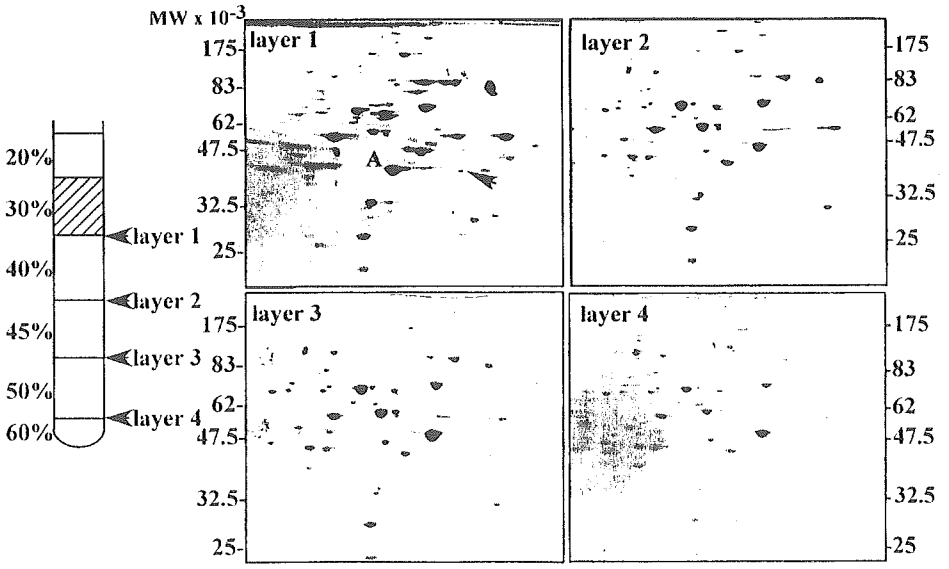

Fig. 5. Subcellular localization of LBP. The membrane proteins recovered from layers 1, 2, 3, and 4 after sucrose density-gradient centrifugation were analyzed by 2-D PAGE. The 2-D gels were stained with CBB. The arrow in the layer 1 gel points to LBP.

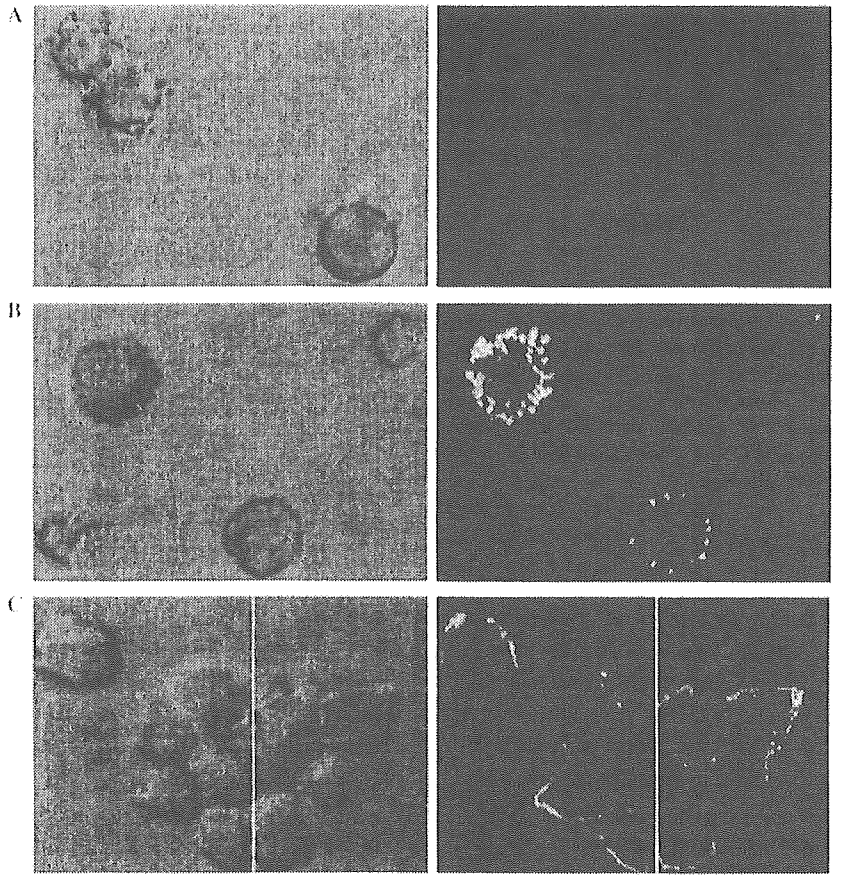

Fig. 6. Immunostaining of mouse and human EC cells with SSEA-4. Phase-contrast micrograph (left) and confocal micrograph (right). (A) Isotype-matched negative control Mab (Raft.1)/mouse EC F9—there is no staining. (B) Raft.2/F9—dot-like surface-staining. (C) Raft.2/human EC NCR-G3—even surface-staining.

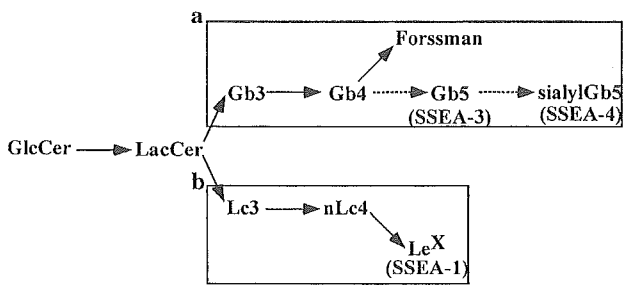

GlcCer:	Glcβ1→Cer
LacCer:	Galβ1,4Glcβ1→Cer
Gb3:	Galα1,4Galβ1,4Glcβ1→Cer
Gb4:	GalNAcβ1,3Galα1,4Galβ1,4Glcβ1→Cer
Forssman:	GalNAcα1,3GalNAcβ1,3Galα1,4Galβ1,4Glcβ1→Cer
Gb5:	Galβ1,3GalNAcβ1,3Galα1,4Galβ1,4Glcβ1→Cer
sialylGb5:	NeuAcα2,3Galβ1,3GalNAcβ1,3Galα1,4Galβ1,4Glcβ1→Cer
Lc3:	GlcNAcβ1,3Galβ1,4Glcβ1→Cer
nLc4:	Galβ1,4GlcNAcβ1,3Galβ1,4Glcβ1→Cer
Le^X:	Galβ1,4(Fucα1,3)GlcNAcβ1,3Galβ1,4Glcβ1→Cer

Fig. 7. Scheme summarizing the major glycosylation pathways in mouse EC F9 cells. The globoseries glycolipid synthesis pathway (a) and the neolactoseries glycolipid synthesis pathway (b) lead to the synthesis of SSEA-3 and -4 and SSEA-1 active glycolipids, respectively. The cells exhibit a distinct pattern of globo- and neolacto-series oligosaccharide chain elongation (solid arrows). Retinoic acid treatment converts the synthesis of Forssman to SSEA-3 and -4 (dotted arrows).

evidence that the SSEA-4 epitope is also carried by a protein, 34/67 laminin receptor, also called LBP.

In culture, the differentiation of murine EC or ES cells into endoderm-like cells is typically characterized by the loss of SSEA-1 expression and the appearance of SSEA-3 and SSEA-4 [14], and may be accompanied by up-regulation of laminin synthesis [15]. Laminins are a family of extracellular matrix proteins that constitute the major non-collagenous glycoproteins found in the basement membrane and are involved in multiple important biological activities, such as assembly of the basement membrane, cell attachment, migration, neurite outgrowth, and angiogenesis [16,17]. In addition, laminins have well demonstrated roles in diverse developmental processes, from the pre-implantation period onwards [18]. Laminin receptors are divided into two major groups: integrin and non-integrin receptors. One of the non-integrin receptors is the mw 67K laminin receptor, LBP [19]. A highly conserved multifunctional mw 37K laminin receptor protein is the precursor of the 67K laminin receptor but the exact manner by which it forms a mature laminin receptor is not clear [20]. Endo and co-workers demonstrated that the glycans of α-dystroglycan include *O*-mannosyl oligosaccharides,

and that a sialyl *O*-mannosyl glycan, Siaα 2,3Galβ1,4GlcNAcβ1,2Man, of α-dystroglycan is a laminin-binding ligand of α-dystroglycan [21,22]. Furthermore, α-dystroglycan from sheep brain has an SSEA-1 structure O-linked to Man [23]. We found that another non-integrin laminin receptor, LBP of human and mouse EC cells, has the SSEA-4 epitope. Since laminin is essential to autocrine- or paracrine-signaling throughout mammalian development and differentiation, the up-regulation of laminin production might have some relationship with SSEA-4 expression on the laminin receptor. However, Raft.2 had no significant effects on F9 cell adhesion to a coverslip precoated with the murine Engelbreth–Holm–Swam tumor-derived laminin (data not shown).

The F9 cell exhibits a distinct pattern of globo- and neolacto-series oligosaccharide chain elongation (Fig. 7). In the globoseries pathway, globotetraosylceramide (Gb4) is not elongated to globopentaosylceramide (Gb5) by the addition of Gal, but rather to the Forssman antigen by the addition of GalNAc [24]. The β1,3-galactosyltransferase-V (β3GalT-V) can catalyze the transfer of Gal not only to GlcNAc-based acceptors with a preference for the core3 O-linked glycan GlcNAc(β1,3)-GalNAc structure, but also to the terminal GalNAc unit of Gb4, thereby leading to the synthesis of Gb5 [25]. These investigators further confirmed that Gb5 synthesis, or SSEA-3 expression in F9 cells is due to β3GalT-V. SSEA-3 synthase, i.e., β3GalT-V, can be said to catalyze Gal addition to both the acceptor of glycolipid and protein. SSEA-4 synthase, which transfers sialic acid to Gb5, was recently cloned from a human renal cancer cell line, ACHN, and the cloned cDNA was found to have a sequence identical to previously cloned α2,3-sialyltransferase (ST3Gal II) [26]. It catalyzes the transfer of sialic acid to the Galβ1,3GalNAc epitope of Gb5 in addition to asialo-GM1 and GM1a [27]. Whether ST3Gal II acts on a proteinous acceptor, such as LBP, is unknown. These transferases, which can glycosylate LBP, should be characterized to elucidate the role of the sugar moiety in differentiation.

Acknowledgments

We thank Ms. S. Yamauchi for her excellent secretarial work, and Drs. Susumu Watanabe and Tomomi Kayamori of Hitachi Science Systems, for mass spectrometric analysis of the Raft.2-binding protein. This work was supported in part by MEXT. KAKENHI 16017321, a grant from the Japan Health Sciences Foundation for Research on Health Sciences Focusing on Drug Innovation KH21014 and also by the CREST grant from the Japan Science and Technology.

References

[1] L.H. Shevinsky, B.B. Knowles, I. Damjanov, D. Solter, Monoclonal antibody to murine embryos defines a stage-specific embryonic antigen expressed on mouse embryos and human teratocarcinoma cells, Cell 30 (1982) 697–705.

[2] N.W. Fox, I. Damjanov, B.B. Knowles, D. Solter, Stage-specific embryonic antigen 3 as a marker of visceral extraembryonic endoderm, Dev. Biol. 103 (1984) 263–266.

[3] P.W. Andrews, Retinoic acid induces neuronal differentiation of a cloned human embryonal carcinoma cell line in vitro, Dev. Biol. 103 (1984) 285–293.

[4] R. Kannagi, E. Nudelman, S.B. Levery, S. Hakomori, A series of human erythrocyte glycosphingolipids reacting to the monoclonal antibody directed to a developmentally regulated antigen SSEA-1, J. Biol. Chem. 257 (1982) 14865–14874.

[5] R. Kannagi, N.A. Cochran, F. Ishigami, S. Hakomori, P.W. Andrews, B.B. Knowles, D. Solter, Stage-specific embryonic antigens (SSEA-3 and -4) are epitopes of a unique globo-series ganglioside isolated from human teratocarcinoma cells, EMBO J. 2 (1983) 2355–23561.

[6] Y.U. Katagiri, K. Ohmi, C. Katagiri, T. Sekino, H. Nakajima, T. Ebata, N. Kiyokawa, J. Fujimoto, Prominent immunogenicity of monosialosyl galactosylgloboside, carrying a stage-specific embryonic antigen-4 (SSEA-4) epitope in the ACHN human renal tubular cell line-a simple method for producing monoclonal antibodies against detergent-insoluble microdomains/raft, Glycoconj. J. 18 (2001) 347–353.

[7] T. Maruyama, A. Umezawa, S. Kusakari, H. Kikuchi, M. Nozaki, J. Hata, Heat shock induces differentiation of human embryonal carcinoma cells into trophectoderm lineages, Exp. Cell Res. 224 (1996) 123–127.

[8] K. Nakamura, M. Suzuki, C. Taya, F. Inagaki, T. Yamakawa, A. Suzuki, A sialidase-susceptible ganglioside, IV3 alpha(NeuGc alpha 2-8NeuGc)-Gg4Cer, is a major disialoganglioside in WHT/Ht mouse thymoma and thymocytes, J. Biochem. 110 (1991) 832–841.

[9] H. Nakajima, Y.U. Katagiri, N. Kiyokawa, T. Taguchi, T. Suzuki, T. Sekine, K. Mimori, H. Nakao, T. Takeda, J. Fujimoto, Single-step method for purification of Shiga toxin-1 B subunit using receptor-mediated affinity chromatography by globotriaosylceramide-conjugated octyl sepharose CL-4B, Protein Exp. Purif. 22 (2001) 267–275.

[10] Y.U. Katagiri, K. Ohmi, W. Tang, H. Takenouchi, T. Taguchi, N. Kiyokawa, J. Fujimoto, Raft.1, a monoclonal antibody raised against the raft microdomain, recognizes G-protein β1 and 2, which assemble near nucleus after Shiga toxin binding to human renal cell line, Lab. Invest. 82 (2002) 1735–1745.

[11] K. Nakamura, Y. Hashimoto, M. Suzuki, A. Suzuki, T. Yamakawa, Characterization of GM1b in mouse spleen, J. Biochem. 96 (1984) 949–957.

[12] R. Kannagi, S.B. Levery, F. Ishigami, S. Hakomori, L.H. Shevinsky, B.B. Knowles, D. Solter, New globoseries glycosphingolipids in human teratocarcinoma reactive with the monoclonal antibody directed to a developmentally regulated antigen, stage-specific embryonic antigen 3, J. Biol. Chem. 258 (1983) 8934–8942.

[13] M. Ozawa, T. Muramatsu, D. Solter, SSEA-1, a stage-specific embryonic antigen of the mouse, is carried by the glycoprotein-bound large carbohydrate in embryonal carcinoma cells, Cell Differ. 16 (1985) 169–173.

[14] J.K. Henderson, J.S. Draper, H.S. Baillie, S. Fishel, J.A. Thomson, H. Moore, P.W. Andrews, Preimplantation human embryos and embryonic stem cells show comparable expression of stage-specific embryonic antigens, Stem Cells 20 (2002) 329–337.

[15] A. van de Stolpe, M. Karperien, C.W. Lowik, H. Juppner, G.V. Segre, A.B. Abou-Samra, S.W. de Laat, L.H. Defize, Parathyroid hormone-related peptide as an endogenous inducer of parietal endoderm differentiation, J. Cell Biol. 120 (1993) 235–243.

[16] K.M. Malinda, K.H. Kleinman, The laminins, Int. J. Biochem. Cell Biol. 28 (1996) 957–959.

[17] K.M. Malinda, M. Nomizu, M. Chung, M. Delgado, Y. Kuratomi, Y. Yamada, H.K. Kleinman, M.L. Ponce, Identification of laminin alpha1 and beta1 chain peptides active for endothelial cell adhesion, tube formation, and aortic sprouting, FASEB J. 13 (1999) 53–62.

[18] J.H. Miner, P.D. Yurchenco, Laminin functions in tissue morphogenesis, Annu. Rev. Cell Dev. Biol. 20 (2004) 255–284.

[19] E.E. Simon, J.A. McDonald, Extracellular matrix receptors in the kidney cortex, Am. J. Physiol. 259 (1990) F783–F792.

[20] S. Buto, E. Tagliabue, E. Ardini, A. Magnifico, C. Ghirelli, F. van den Brule, V. Castronovo, M.L. Colnaghi, M.E. Sobel, S. Menard, Formation of the 67-kDa laminin receptor by acylation of the precursor, J. Cell. Biochem. 69 (1998) 244–251.

[21] A. Chiba, K. Matsumura, H. Yamada, T. Inazu, T. Shimizu, S. Kusunoki, I. Kanazawa, A. Kobata, T. Endo, Structures of sialylated O-linked oligosaccharides of bovine peripheral nerve alpha-dystroglycan. The role of a novel O-mannosyl-type oligosaccharide in the binding of alpha-dystroglycan with laminin, J. Biol. Chem. 272 (1997) 2156–2162.

[22] T. Sasaki, H. Yamada, K. Matsumura, T. Shimizu, A. Kobata, T. Endo, Detection of O-mannosyl glycans in rabbit skeletal muscle alpha-dystroglycan, Biochim. Biophys. Acta 1425 (1998) 599–606.

[23] N.R. Smalheiser, S.M. Haslam, M. Sutton-Smith, H.R. Morris, H.R.A. Dell, Structural analysis of sequences O-linked to mannose reveals a novel Lewis X structure in cranin (dystroglycan) purified from sheep brain, J. Biol. Chem. 273 (1998) 23698–23703.

[24] J.G. Krupnick, I. Damjanov, A. Damjanov, Z.M. Zhu, B.A. Fenderson, Globo-series carbohydrate antigens are expressed in different forms on human and murine teratocarcinoma-derived cells, Int. J. Cancer 59 (1994) 692–698.

[25] D. Zhou, T.R. Henion, F.B. Jungalwala, E.G. Berger, T. Hennet, The beta 1,3-galactosyltransferase beta 3GalT-V is a stage-specific embryonic antigen-3 (SSEA-3) synthase, J. Biol. Chem. 275 (2000) 22631–22634.

[26] S. Saito, H. Aoki, A. Ito, S. Ueno, T. Wada, K. Mitsuzuka, M. Satoh, Y. Arai, T. Miyagi, Human alpha2,3-sialyltransferase (ST3Gal II) is a stage-specific embryonic antigen-4 synthase, J. Biol. Chem. 278 (2003) 26474–26479.

[27] Y.J. Kim, K.S. Kim, S.H. Kim, C.H. Kim, J.H. Ko, I.S. Choe, S. Tsuji, Y.C. Lee, Molecular cloning and expression of human Gal beta 1,3GalNAc alpha 2,3-sialytransferase (hST3Gal II), Biochem. Biophys. Res. Commun. 228 (1996) 324–327.

Cell Separation Between Mesenchymal Progenitor Cells Through Porous Polymeric Membranes

Akon Higuchi,[1] Yosuke Shindo,[1] Yumiko Gomei,[1] Taisuke Mori,[2] Taro Uyama,[2] Akihiro Umezawa[2]

[1]Department of Applied Chemistry, Seikei University, 3-3-1 Kichijoji Kitamachi, Musashino, Tokyo 180-8633, Japan

[2]Department of Reproductive Biology and Pathology, National Center for Child and Development, Setagaya, Tokyo 154-8567

Received 9 August 2004; revised 5 October 2004; accepted 12 October 2004
Published online 19 May 2005 in Wiley InterScience (www.interscience.wiley.com). DOI: 10.1002/jbm.b.30220

Abstract: This study investigates the separation of two types of marrow stromal cells, KUSA-A1 osteoblasts and H-1/A preadipocytes, by filtration through various porous polymeric membranes. It was found that KUSA-A1 permeates better than H-1/A cells through 12-μm polyurethane foaming membranes. This appears to be due to the relatively smaller cell size of KUSA-A1 cells. In addition, when feed solutions containing suspensions of either cell type or a mixture of the two were used, the permeation ratio was relatively low (< 6%) through polyurethane and surface-modified polyurethane foaming membranes. It was also found that there was some degree of separation between KUSA-A1 and H-1/A cells (separation factor = 1.8) with nylon-net filter membranes, but no separation was obtained when filters made of nonwoven fabrics or silk screens were used. This ability of the nylon-net filter membranes to separate the two cell types was due to a sieving effect that results from an optimal pore size. Finally, permeation of a solution of human serum albumin through the membrane following filtration of the cells did not result in a separation of cells in the recovery solution. © 2005 Wiley Periodicals, Inc. J Biomed Mater Res Part B: Appl Biomater 74B: 511–519, 2005

Keywords: cell separation; mesenchymal progenitor cells; flow cytometry; biomaterials; polyurethane foaming membrane

INTRODUCTION

Bone-marrow stromal cells make up the microenvironment of the bone marrow and are required for the generation of multipotent stem cells.[1] In addition, bone-marrow stromal cells have many characteristics of mesenchymal stem cells, which produce progeny that can differentiate into multiple cell lineages. Pluripotent stem cells derived from marrow stroma can differentiate into several cell types, including bone, cartilage, fat, tendon, and muscle. Recent studies also show that the marrow stroma may be a potential source of cardiomyocytes.[2]

Purification and isolation of specific mesenchymal cells are necessary to obtain bone-marrow stromal cells for use in clinical applications. For example, it is necessary to generate cardiomyocytic progenitors from marrow stroma for the treatment of heart failure by cell transplantation into damaged myocardia. Thus, a method is needed for the separation and isolation of specific mesenchymal cells from bone-marrow stromal cells. Cell separation can be accomplished by centrifugation,[3,4] fluorescence-activated cell sorting (FACS),[5] magnetic cell selection,[6–9] affinity chromatography,[10,11] or membrane filtration.[12–14] Of these methods, membrane filtration method is a good candidate for the purification of mesenchymal cells because it is simple and inexpensive and because it is easy to maintain sterility during the filtration process. In fact, a previous study[14] showed that $CD34^+$ cells could be purified by filtration through chemically modified 5-μm-pore polyurethane (PU) membranes.

Here the separation of cells from a mixture of KUSA-A1 and H-1/A cells with the use of membrane filtration is reported. The goal of this study was to find the optimal membrane type (membrane pore size, morphology, and material) and filtration conditions for the isolation of marrow stromal cells.

MATERIALS AND METHODS

Materials

Base membranes used for the chemical modification were porous PU foaming membranes (Ruby Cell S, Toyo Polymer Co., Ltd.). Porous PU foaming membranes containing 0.61% of epoxy group (PU-epoxy) were prepared by plasma polymerization with glycidylmethacrylate after the membranes were plasma discharged at 200 W for 30 s under 0.2 torr of Ar gas.[14] The average pore size of the PU

Correspondence to: Akio Higuchi (e-mail: higuchi@ch.seikei.ac.jp)
Contract grant sponsor: Ministry of Education, Culture, Sports, Science, and Technology of Japan Grant-in-Aid for Scientific Research on Priority Areas (B, "Novel Smart Membranes Containing Controlled Molecular Cavity"); contract grant number: 13133202
Contract grant sponsor: Salt Science Foundation
Contract grant sponsor: Asahi Glass Foundation

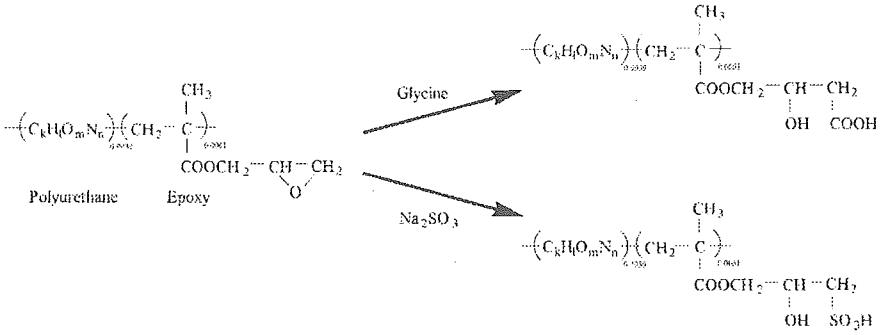

Scheme 1

and PU-epoxy membranes evaluated from capillary flow porometer measurements (Porous Materials, Inc.) was 12 μm. The PU and PU-epoxy membranes had 86% porosity and 1.2-mm thickness.

Nylon-net filters [NY11 (pore size = 11 μm), Millipore Corporation], two kinds of nonwoven fabrics having fine fiber diameter for cleaning lenses made of acrylonitrile (Cleaning lens, No Brand Co.) and nylon + polyester (La Clean, 3052-01, Nagoya Glass Co.), and silk screens made of silk (No. 150, Nihon Zokei Co.) and Tetron™ (Nos. 150 and 250, Nihon Zokei Co.) were also used for the cell separation, where "No." indicates number of fibers per inch.

Human serum albumin (HSA, 019-10503, Wako Pure Chemical Industries) was used as received. Cell Tracker Orange™ (C-2927, Molecular Probes, Inc.) and Cell Tracker Green™ (C-2925, Molecular Probes, Inc.) were used as received. Other chemicals, purchased from Tokyo Chemical Co., were reagent grade and were used without further purification. Ultrapure water was used throughout the experiments.

Preparation of Surface-Modified Membranes

Sulfonic acid and carboxylic acid groups were introduced from the opening reaction of the epoxy group on the PU-epoxy membranes, followed by the reaction between the epoxy group and H_2SO_4 or glycine reported in the literature.[14–16] Reaction conditions are reported in the literature.[14] The product anticipated to result from the ring-opening reaction of the epoxy group is shown in Scheme 1.[14] The resultant membranes were referred to as PU-SO_3H and PU-COOH membranes. After the reaction, the surface-modified PU membranes were rinsed in ultrapure water for 3 h, and stocked in ultrapure water at 4°C.

Cell Culture

Mesenchymal progenitor cell lines, KUSA-A1 and H-1/A, derived from the bone marrow of C3H/He and C57/Bl mice, respectively,[1,2] were maintained in DMEM media (D5648, Sigma-Aldrich, Japan K.K.) supplemented with 100 mg/L streptomycin sulfate (196-08511, Wako Pure Chemical Industry, Ltd.), 70 mg/L benzylpenicillin potassium (023-07731, Wako Pure Chemical Industry, Ltd.) and 10% fetal bovine serum (FBS, JRH Bioscience). KUSA-A1 and H-1/A cells were expanded by standard cell culture techniques[17–19] in 75-cm^2 tissue-culture flasks containing 40 mL of 10% serum-supplemented medium in a CO_2 incubator (BNA-111, Espec Co.) in 5% CO_2 atmosphere at 37°C.

The cell number was characterized by observation of the cells with an inverted microscope (Diaphoto TMD300, Nikon Co.) equipped with a CCD video camera, ARGUS 20 (Hamamatsu Photonics K.K.) and a temperature-regulated box.

Cell Dying with Cell Tracker

KUSA-A1 cells and H-1/A cells were dyed with Cell Tracker™ (Cell Tracker Orange™ and Cell Tracker Green™, respectively) in order to mark each cell in flow-cytometry analysis. A quantity of 1 mg Cell Tracker Orange™ was dissolved in 1 mL of methanol, and the Cell Tracker Orange™ solution was aliquotted into 20 samples (50 μL). A quantity of 50 μg Cell Tracker Green™ was dissolved in 0.5 mL of dimethylsulfoxide, and the Cell Tracker Green™ solution was aliquotted into 10 samples (50 μL). The Cell Tracker Orange™ and Cell Tracker Green™ solutions were stored under −20°C. The cell dying with Cell Tracker Orange™ and Cell Tracker Green™ was performed as follows:

1. A quantity of 50 μL of Cell Tracker solution was pipetted into 5 mL of 10% serum-supplemented DMEM medium.
2. The medium was decanted off, and the cells were rinsed with 10 mL phosphate-buffered solution (PBS).
3. The PBS was decanted off and the Cell Tracker™ solution was pipetted into the tissue-culture flask. The cells in the tissue-culture flask were incubated in a 5% CO_2 atmosphere for 30 min at 37°C.
4. The Cell Tracker™ medium was decanted off and the cells were subsequently rinsed with a quantity of 10 mL PBS solution. Twenty milliliters of 10% serum-supplemented DMEM medium was pipetted into the tissue-culture flask after the PBS solution was decanted off, and the cells in the tissue-culture flask were again incubated in a 5% CO_2 atmosphere for 30 min at 37°C.
5. Step 4 was performed in duplicate.
6. After incubation, the DMEM medium was decanted off and a quantity of 10 mL PBS solution was added to the tissue-culture flask in order to rinse the cells.
7. A quantity of 4 mL of trypsin in PBS solution was pipetted into the tissue-culture flask after the PBS solution was decanted off. After 5 min, the trypsin solution was decanted off and a quantity of 5 mL of DMEM medium was added to the tissue-culture flask. The cells on the bottom of the culture flask were resuspended in the DMEM medium by gently pipetting up and down.
8. The cell suspension was centrifuged at 130 rpm for 3 min. The supernatant was carefully decanted off, and 7 mL of fresh DMEM medium was added to the cells.